

Petroleum Diesel-Assisted Ambient Temperature Aqueous-Nonaqueous Hybrid Bitumen

Extraction Process

by

Derek Russell

A thesis submitted in partial fulfillment of the requirements for the degree of

Master of Science

in

Chemical Engineering

Department of Chemical and Materials Engineering  
University of Alberta

©Derek Russell, 2017

## **Abstract**

Solvents are used in the oil sands industry to reduce the viscosity of bitumen and hence to assist recovery of bitumen prior to its upgrading. Solvents can also be added to the ores to reduce energy consumption during the aqueous-nonaqueous hybrid bitumen extraction process at ambient conditions. The interfacial tension and zeta potential of petroleum diesel in water were measured to confirm the presence of surface active chemicals in petroleum diesel. Functional groups of the surface active species were found to be present in petroleum diesel using fourier transform infrared spectroscopy and gas chromatography mass spectrometry techniques. The characterization techniques confirmed the presence of aliphatic compounds and aromatic compounds in the petroleum diesel, which make petroleum diesel an effective solvent as process aids for bitumen extraction from oil sands ores. Different ores were used at various petroleum diesel dosages to evaluate the performance/efficiency of petroleum diesel on bitumen extraction process from the selected types of ores. The overall extraction performance of selected ores was improved as more petroleum diesel was added to the ores prior to the batch extraction process. The addition of petroleum diesel led to higher initial rates of bitumen liberation and decreased induction time for bitumen and air bubble attachment. The results showed that the optimum addition of petroleum diesel is approximately 10% by mass of bitumen in ore.

Dodecane was used as a model solvent to estimate the loss of petroleum diesel to tailings using thermogravimetric analysis techniques. The solvent loss was found to meet the specification of 4 barrels of solvent per 1000 barrels of bitumen produced. Both petroleum diesel and dodecane showed similar impact on bitumen extraction from oil sands ores. The bitumen liberation analysis showed that the reduction of bitumen viscosity is the main factor for improving bitumen

recovery in the aqueous-nonaqueous hybrid bitumen extraction process. The similar performance between petroleum diesel and dodecane indicates that the natural surfactants of petroleum diesel did not play a strong role in improving the bitumen extraction from oil sands ores.

The reduction in viscosity of bitumen facilitates the migration of bitumen natural surfactants to the interface as shown by lower interfacial tensions between bitumen and water, which play a strong role in bitumen liberation process.

## **Acknowledgements**

I would like to give thanks to my supervisors, Dr. Zhenghe Xu and Dr. Qingxia (Chad) Liu for their valuable guidance and great support, including their feedback and constructive criticism on the progress of my thesis project. Their passions in the scientific field motivated me to excel academically on my thesis project.

Thanks to Mr. Yeling Zhu for his valuable guidance and encouragement in the progress of my thesis project. Also, our discussions helped me successfully plan my research on evaluating solvents for novel concept of hybrid bitumen extraction process.

I would also like to give Ms. Lisa Carreiro, Ms. Patricia Siferd, and Mr. Carl Corbett thanks for their administrative services and support to our research teams. I would also like to thank Mr. Jim Skwarok and Ms. Jie Ru for their technical support in the laboratory environment and for providing me training sessions on how to use the lab equipment. I would also like to express my great appreciation to Dr. Lan Liu for conducting GC/MS experiments on my behalf.

Finally, I would like to express my gratitude to members of Dr. Xu and Dr. Liu's research groups for their valuable guidance, discussion, support and being patient with me while improving my communication skills.

Lastly, the financial support from the National Sciences and Engineering Research Council of Canada (NSERC) was greatly appreciated. I would like to express my gratitude to a number of industrial professionals for their technical and financial support to our research teams.

# Table of Contents

Table of Contents .....	v
List of Tables .....	vii
List of Figures .....	viii
Chapter 1: Introduction .....	1
1.1 The Oil Sands of Canada .....	1
1.1.2 Economical Demand .....	2
1.2 Bitumen Extraction Process .....	3
1.2.1 In Situ Operation .....	4
1.2.2 Aqueous Extraction Process (Surface Mining) .....	4
1.2.3 Tailings .....	6
1.3 Challenges in Current Aqueous Extraction Processes .....	7
1.4 Thesis Objectives .....	9
1.5 Thesis Outline .....	10
Chapter 2: Literature Review .....	12
2.1 Characterization of Ores .....	12
2.2 Key Process Parameters .....	12
2.2 Interfacial Phenomena .....	14
2.3 Colloids .....	15
2.4 Extraction Sub-Processes .....	18
2.4.1 Liberation Process .....	19
2.4.2 Aeration Process .....	21
2.5 Chemical Process Aids .....	22
2.6 Petroleum Diesel .....	23
Chapter 3: Research Methodology .....	25
3.1 Petroleum Diesel (Commercial Fuel) .....	25
3.2 Characterization of Oil Sands Ores .....	26
3.3 Extraction Process Water and Mineralogy of Fines .....	26
3.2 Experimental Methods .....	28
3.3.1 Gas Chromatography/Mass Spectrometry (GC-MS) .....	28

3.3.2 Fourier Transform Infrared Spectroscopy .....	28
3.2.3 Tensiometry .....	28
3.2.4 Electrophoresis .....	29
3.3.5 Batch Extraction Test Procedure .....	30
3.3.6 Optical Microscopy .....	32
3.3.7 Custom Designed Induction Timer Device .....	34
Chapter 4: Results and Discussion - Characterization of Petroleum Diesel .....	37
4.1 Composition of Petroleum Diesel .....	37
4.2 FTIR Spectrum of the Petroleum Diesel Sample .....	41
4.3 Surface and Interfacial Tension of Petroleum Diesel and Deionized Water .....	43
4.4 Interfacial Tension between Petroleum Diesel and Deionized Water at Different pH .....	45
4.5 Zeta Potential of Emulsified Petroleum Diesel in Electrolyte Solutions .....	47
Chapter 5: Results and Discussion – Industrial Research .....	49
5.1 Bitumen Viscosity .....	49
5.2 Batch Bitumen Extraction Process .....	50
5.3 Comparison between Petroleum Diesel and Dodecane .....	55
5.4 Bitumen Liberation Process .....	57
5.4 Bitumen Aeration Process .....	59
Chapter 6: Solvent Loss to Tailings .....	62
6.1 Objective .....	62
6.2 Preliminary Experiment (Petroleum Diesel) .....	62
6.3 Method of Solvent Loss Analysis .....	63
6.3 Results and Discussion .....	64
6.4 Conclusions .....	69
Chapter 7: Conclusions .....	70
Chapter 8: Contribution to Original Knowledge .....	72
Chapter 9: Future Research .....	72
References .....	74

## List of Tables

Table 3.1: Specifications of petroleum diesel used in thesis project (Shell Canada) .....	25
Table 3.2: Composition of oil sands ores used for the study .....	26
Table 3.3: Composition of Aurora process water determined by ion chromatography .....	27
Table 3.4: Mineralogy composition of fine particles by x-ray diffraction .....	27
Table 4.1: Chemical composition of petroleum diesel containing heteroatoms .....	40
Table 4.2: Surface tension and interfacial tension .....	44
Table 6.1: Summary of dodecane in froth determined by TGA .....	68
Table 6.2: Summary in loss of dodecane to tailings solids .....	68

## List of Figures

Figure 1.1: Schematic diagram of the proposed oil sands structural model, developed by Takamura .....	2
Figure 1.2: Demand of synthetic crude oil and non-upgraded bitumen .....	3
Figure 1.3: General diagram for aqueous-based bitumen extraction process .....	5
Figure 1.4: Tailing ponds at Suncor facility near Fort McMurray, Alberta .....	6
Figure 2.1: Schematic diagram of the calcium binder between bitumen and fines solids .....	13
Figure 2.2: Effect of temperature on induction time for air bubble-bitumen attachment .....	14
Figure 2.3: Normalized Gibbs free energy of particle interactions versus distance for two identical spherical particles with radius of 100 nm in water, containing different concentration of monovalent salt .....	16
Figure 2.4: Typical diagram of Gouy-Chapman-Stern model .....	18
Figure 2.5: Schematic diagram of a bitumen droplet on solids in water .....	20
Figure 2.6: Schematic diagram of aeration process of bitumen .....	22
Figure 2.7: Simple model of naphthenic acid .....	24
Figure 3.1: Schematic diagram of the tensiometer (Du Nouy ring) .....	29
Figure 3.2: Photograph of Denver flotation extraction used in this study .....	32
Figure 3.3: Photograph of optical microscope for visualization of bitumen liberation process ..	33
Figure 3.4: Schematics of a custom designed induction timer for aeration experiments .....	35
Figure 3.5: Apparatus for preparation of fines-coating on bitumen .....	36
Figure 4.1: Thermogravimetric curve of petroleum diesel. ....	38
Figure 4.2: Total ion chromatograms for the evaporated petroleum diesel at 500 °C .....	39
Figure 4.3: FTIR spectrum of the petroleum diesel sample .....	42
Figure 4.4: FTIR spectrum of petroleum diesel and commercial surfactant salts .....	43
Figure 4.5: Dynamic interfacial tension between petroleum diesel and deionized water. ....	45
Figure 4.6: Interfacial tension between petroleum diesel and water as a function of pH .....	46
Figure 4.7: Zeta potential of emulsified petroleum diesel as a function of pH in 10 mM KCl solution .....	48
Figure 5.1: Effect of petroleum diesel dosage on bitumen viscosity (courtesy of Yeling Zhu) ...	50
Figure 5.2: Photographs of froth from AC ore in process water slurry (a) 0 wt.% (b) 5 wt.% diesel (c) 10 wt.% diesel (d) 20 wt.% diesel .....	51
Figure 5.3: Extraction results to evaluate the performance of petroleum diesel for bitumen extraction .....	53
Figure 5.4: Distribution of hydrocarbon (bitumen and petroleum diesel), water, and solids in froth .....	54
Figure 5.5: Extraction results for AC Ores using standard Denver Cell experimental protocol. .	56
Figure 5.6: Comparison of solvent effect on froth composition of AC Ores during extraction process .....	56
Figure 5.7: Liberation profiles of ores in Aurora process water at T = 25 °C and pH of 7.52. ....	57



Figure 5.8: Effect of solvent dosage on liberation performance of various ores .....	59
Figure 5.9: Probability profile of air bubble-bitumen attachment over the contact time between bitumen and air bubble.....	60
Figure 5.10: Induction time as a function of petroleum diesel dosage .....	60
Figure 5.11: Comparison of aeration process between bitumen and fines-coated bitumen. ....	61
Figure 6.1: TGA profile of solids and hydrocarbon sample (~2 wt.% petroleum diesel and ~8 wt.% bitumen).....	62
Figure 6.2: Typical schematic diagram of the TGA apparatus.....	64
Figure 6.3: TGA profile of AC solid soaked with solvent.....	65
Figure 6.4: TGA profile of AC solid sample.....	66
Figure 6.5: TGA profile of (a) primary froth and (b) tailings solids produced during extraction (20 wt.% dodecane case).....	67

# Chapter 1: Introduction

## 1.1 The Oil Sands of Canada

Oil sands are a mixture of bitumen, mineral solids, and water. Canada has one of the largest reserves of crude oil, second only to Saudi Arabia and accounting for approximately 15% of the world oil reserves.<sup>1</sup> The typical composition of the oil sands in Canada is 85 wt.% mineral solids, 10 wt.% bitumen, and 5 wt.% connate water. The oil deposits in Alberta are located in Athabasca, Wabasca, Peace River, and Cold Lake regions.<sup>2</sup>

The most valuable component of oil sands is the bitumen, which can be upgraded to variety of products such as gasoline, kerosene, petroleum diesel, and asphalt. There exist two common methods for extracting bitumen from oil sands: in-situ and surface mining methods. The Athabasca oil sands contain a thin layer of connate water (~10 nm), which separates the bitumen from solids.<sup>2</sup> This is one of the main reasons why the aqueous extraction method is effective for recovering bitumen from oil sands.

Figure 1.1 shows a schematic diagram of the refined oil sands model developed by Takamura.<sup>2</sup> The sands in the Athabasca region are hydrophilic, which makes it easier for hydrophobic bitumen to detach from the sands during the liberation sub-process of the aqueous bitumen extraction process.

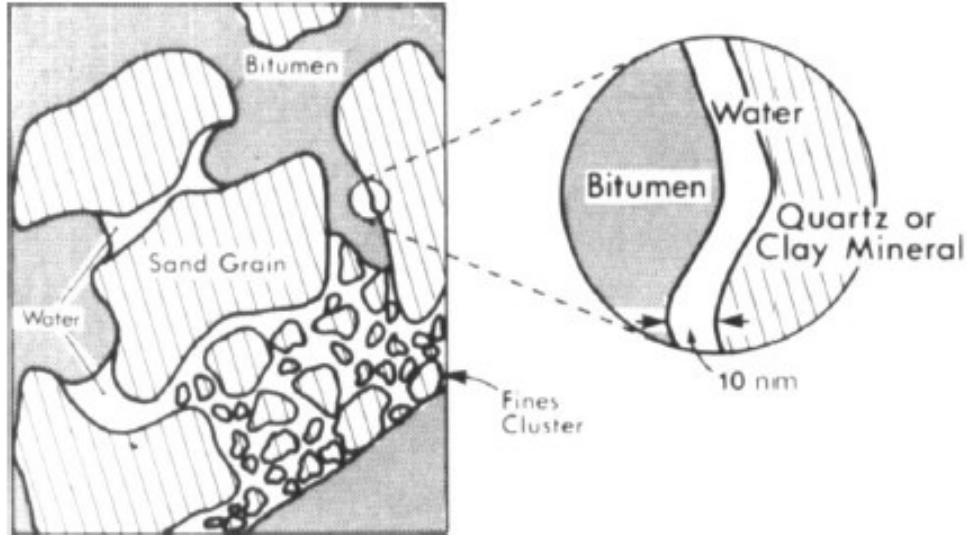


Figure 1.1: Schematic diagram of the proposed oil sands structural model, developed by Takamura.<sup>2</sup>

### 1.1.2 Economical Demand

The demand for petrochemical products is expected to increase over the next several decades due to increased standards of living in developing countries and emerging economies in China and India, which typically results in increased energy consumption.<sup>3</sup> The unconventional oils, characterized by high density and viscosity, are major liquid fossil fuel resources in Canada, which helps provide a security for energy resources in the future.<sup>3</sup> Canada has one of the most abundant crude oil reserves, accounting for 15% of the world total reserves.<sup>4</sup> There are between 1.7 and 2.5 trillion barrels of total bitumen in place in Alberta, which are mainly located in the Athabasca, Peace River and Cold Lake regions.<sup>5</sup> Open pit mining and in-situ technologies are suitable for recovering 300 billion barrels of bitumen in Alberta.<sup>5</sup> In 2012, there were 1.6 million barrels/day (bbl/d) of bitumen produced from Alberta oil sands reserves, of which surface mining method accounted for 50% of the bitumen production.<sup>4</sup>

As shown in Figure 1.2, Alberta Energy Regulator estimated that the demand for upgraded and non-upgraded bitumen exporting to other countries including the United States will increase by 56.4% and 70.6%, respectively, over the next decade.<sup>6</sup> Non-upgraded crude bitumen is transported by the pipelines or rails to the United States for upgrading.<sup>6</sup>

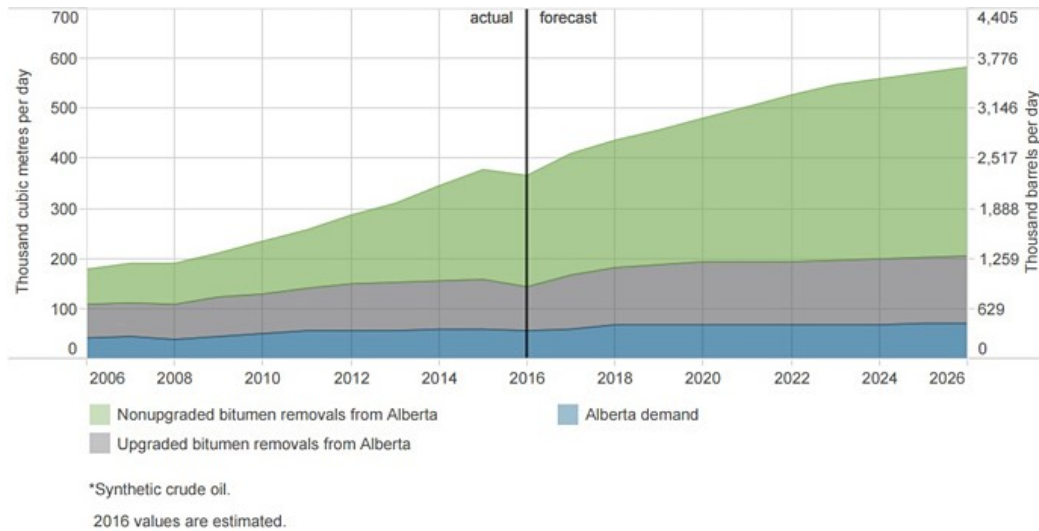


Figure 1.2: Demand of synthetic crude oil and non-upgraded bitumen.<sup>6</sup>

## 1.2 Bitumen Extraction Process

There exist various methods to separate bitumen from the oil sands matrix. For example, Karl Clark developed a hot water extraction method (CHWE), which extracts bitumen from oil sands using hot water and caustic soda (sodium hydroxide) addition at temperature of 70-80 °C.<sup>5,7</sup> This extraction method requires a high level of energy consumption to heat the aqueous slurry. Solvent extraction and pyrolysis (non-aqueous) processes are applied to some oil sands ores in the United States where aqueous extraction process is not suitable due to increased hydrophobicity of solids in the ores.<sup>8</sup> These processes do not require water, but one drawback of the pyrolysis extraction process is the high temperature requirement. The common extraction methods for the production of bitumen in Canada are discussed in the following sections.

### **1.2.1 In Situ Operation**

The in situ operation works well to recover bitumen from oil sands deposits deeper than 70 m below the ground surface. There are several common methods of in situ operations including steam-assisted gravity drainage (SAGD) and cyclic steam stimulation (CSS). In SAGD operation, the latent heat from steam is supplied using a horizontal well to the formation to reduce the viscosity of bitumen, which can then be pumped to the surface.<sup>9</sup> However, this method is challenging due to both high energy and water requirements. In the CSS operation, high pressure steam is applied to provide both latent and sensible heat that mechanically breaks reservoir rocks down and reduces the viscosity of bitumen, which can then be transferred to the production well using the solution gas.<sup>10</sup> Although the in situ method can be used to recover bitumen from the deeper formations, the surface mining method is commonly employed in the Canadian oil sands industries for shallow formations.

### **1.2.2 Aqueous Extraction Process (Surface Mining)**

Figure 1.3 shows a schematic diagram for aqueous extraction of bitumen from oil sands. Ores are collected using large shovels and trucks. Recycled process water is added to the lumps of oil sands to allow conditioning in a mixing unit such as a rotary breaker.<sup>5</sup> In the early 1990's, the hydrotransport pipeline was introduced into the extraction system instead of tumblers to reduce greenhouse gas emissions and operating costs by reducing the current operating temperature to 50 °C from 80 °C. Air and chemical additives are usually introduced in the hydrotransport pipeline to liberate bitumen from oil sand ores and aerate the bitumen.<sup>5</sup>

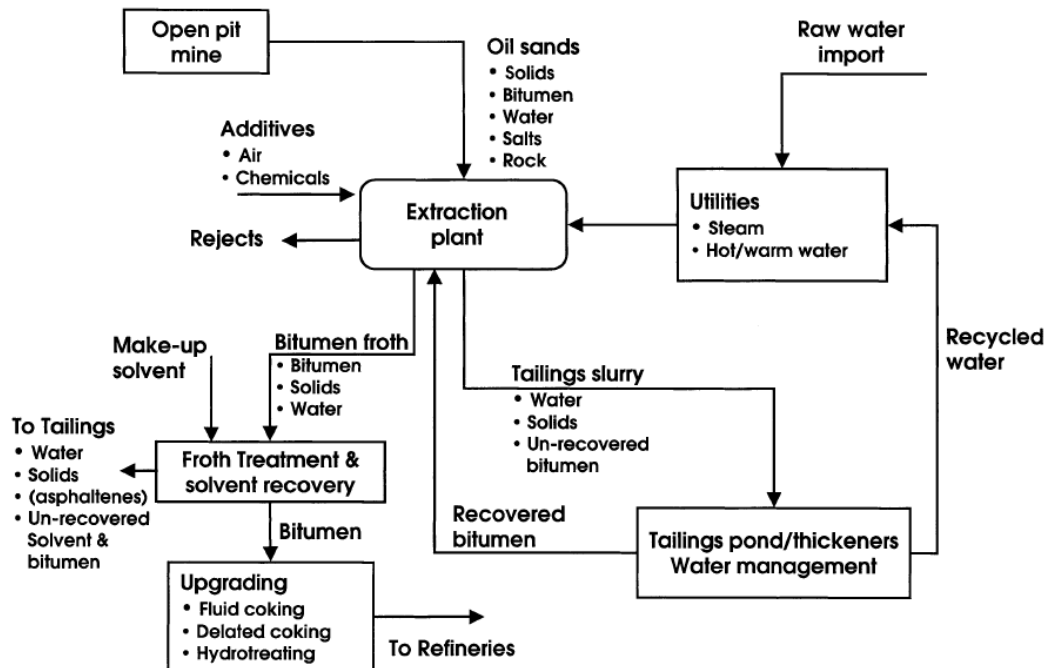


Figure 1.3: General diagram for aqueous-based bitumen extraction process.<sup>5</sup>

The conditioned slurry is transferred to the primary separation vessels (PSV) where most of bitumen floats to the top while heavier components (mainly mineral solids) and unrecovered bitumen settle to the bottom by gravity. The middling layer containing trace of bitumen droplets is transferred to mechanical flotation units in order to recover more bitumen. Froth from both the PSV and secondary mechanical flotation units is combined and passed over to the froth treatment units where solvents, commonly hexane or naphtha, are added to reduce bitumen viscosity and increase density difference for separation of remaining solids and water in order to meet the specification for the upgrading process.<sup>5,11</sup>

Incline plate settlers, cyclone, and centrifuges are common methods used to remove water and solids from diluted bitumen.<sup>5</sup> A paraffinic solvent (e.g. hexane) is used at the Albian froth treatment process to precipitate asphaltenes for efficient removal of water and solids through

aggregation and gravity settling mechanisms. Tailings from the bottom of the key extraction process units can be treated with flocculant or coagulant in the thickener to consolidate mineral solids and release process water for recycling back to the hydrotransport pipeline to reduce the intake of fresh water.<sup>5</sup>

### 1.2.3 Tailings

Tailings are a mixture of mineral solids, water, and unrecovered bitumen. One m<sup>3</sup> of extracted bitumen results in 7.5 m<sup>3</sup> of waste tailings during the extraction process, which results in one of the largest mine tailings storage units in the world.<sup>12</sup> Approximately 795,000 m<sup>3</sup> of process water is used and 954,000 m<sup>3</sup> of tailings is produced each year. A major concern of the process water is the presence of naphthenic acids, which are harmful to aquatic environments.<sup>12</sup> The dyke structures of the tailing ponds are developed using coarser solids of primary tailings to protect the tailing ponds. Figure 1.4 shows an example of the tailing ponds at the Suncor operating facility.

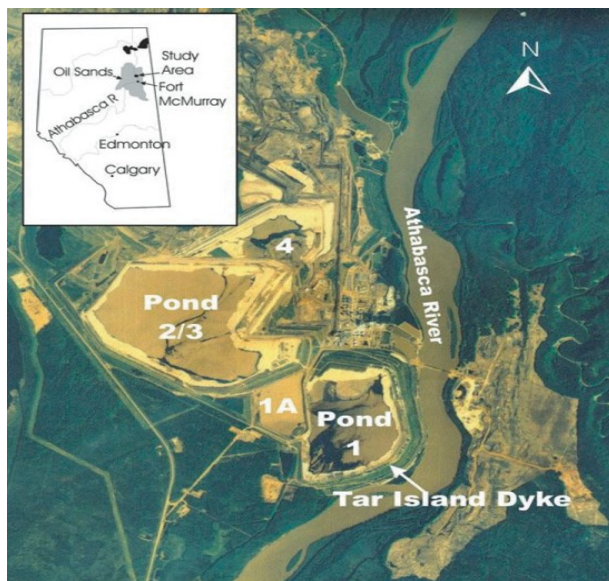


Figure 1.4: Tailings ponds at Suncor facility near Fort McMurray, Alberta.<sup>12</sup>

The inventory of the tailings ponds is expected to increase over the next a number of years. The mining industry is now required by provincial legislation to begin eliminating the storage of fluid tailings and to maximize process water recycle for reducing fresh water consumption and improving the energy efficiency of the extraction process while achieving objectives under the Directive 074 created by Energy Resource Conservation Board in 2009.<sup>13</sup>

The coarse sands in the tailings settle quickly whereas the mature fine tailings (MFT) contains 30 wt.% unsettled solids for a number of years. There are several technologies that are implemented to solve the challenges of mature fine tailings. For example, gypsum is added to consolidate tailings solids and allow release of process water.<sup>13</sup> The novel polymer, Al-PAM (hybrid Al(OH)<sub>3</sub> polyacrylamide), is used for flocculation of oil sands tailings and dewatering; this has the potential to reduce the inventory of the MFT.<sup>14</sup> The stages for dewatering process of MFT involve flocculation and thickening of diluted MFT, followed by filtration of the thickener underflow to produce a dried filter cake, which can then be stacked. This process helps maximize the recycle of process water.<sup>14</sup>

### **1.3 Challenges in Current Aqueous Extraction Processes**

There are several major challenges in the oil sands industry. The aqueous extraction process requires 3 to 4 barrels of water for production of 1 barrel of crude bitumen.<sup>8</sup> A high energy consumption is required to increase the operating temperature of the extraction process due to the high thermal capacity of water, resulting in the generation of greenhouse gas emissions. The introduction of a carbon tax in 2017 by the Government of Alberta increases the operation costs on extraction due to high natural gas consumption for heating aqueous slurry to current operating temperatures of 50 °C. The usage of caustic soda (sodium hydroxide) results in the accumulation of dispersed fine clay particles in the slurry water, which leads to increased accumulation of



tailings ponds over time.<sup>15</sup> The main purpose of sodium hydroxide is to deprotonate the natural surfactants of bitumen to aid the liberation process of bitumen from ores.<sup>16</sup> However, this leads to the increased solubility of natural surfactants and accumulation into the tailings ponds.

The main objective of the oil sands industry is to maximize bitumen recovery while minimizing energy consumption and fresh water input through usage of recycle process water from tailings ponds. Another key objective is to minimize the use of sodium hydroxide to reduce accumulation of mature fines tailings over time. There are several methods employed to overcome the above challenges, including the ionic liquid-assisted solvent extraction and the non-aqueous extraction.

In the ionic liquid-assisted solvent extraction of bitumen, 1-ethyl-3-methyl imidazolium tetrafluoroborate was used in combination with n-heptane and acetone solvent mixtures for extracting bitumen from oil sands. Such combination resulted in a high bitumen recovery of around 90% at room temperature.<sup>17</sup> This method is not commercially feasible due to high cost of the ionic liquid materials.<sup>18</sup>

The total recovery of bitumen was at least 80% during the experimental single stage of the non-aqueous extraction process at room temperature using toluene, cyclopentane, and mixture of n-pentane and cyclopentane at a solvent to bitumen mass ratio of at least 4.<sup>8</sup> Even though the non-aqueous extraction method is effective for recovering bitumen from oil sands without water supply requirements, there are some issues in using these hydrocarbon solvents due to volatility, flammability, and toxicity.<sup>18</sup> It is difficult to treat and remove large amount of solvents from residual sands, the specification for solvent loss to tailings is restricted to less than 4 barrels of solvent per 1000 barrels of bitumen produced.<sup>8</sup> Furthermore, a key objective of the current Athabasca oil sands operation is to achieve bitumen recovery of more than 90%.

The novel concept of aqueous-nonaqueous hybrid bitumen extraction process was developed by Xu et. al. In this process, kerosene is used as a solvent for the pre-treatment of ores prior to the hydrotransport pipeline to reduce the energy consumption by lowering the operating temperature from 50 °C to between 25 and 35 °C.<sup>19</sup> Previously, research was conducted on the use of naphtha and toluene as the solvent, although these solvents cannot be applied commercially due to their high volatility.<sup>20</sup> The results of this research provided insight to the possibility that petroleum diesel may be used as a solvent for aqueous-nonaqueous hybrid bitumen extraction process since petroleum diesel is stable under ambient condition and contains a mixture of aliphatic and aromatic hydrocarbon compounds which can reduce the bitumen viscosity and improve the miscibility of petroleum diesel in bitumen to achieve an optimal bitumen recovery at ambient conditions.

#### **1.4 Thesis Objectives**

The main objective of the thesis research project was to explore the use of petroleum diesel as a solvent for bitumen extraction to evaluate the novel concept of the aqueous-nonaqueous hybrid bitumen extraction process. Another objective was to gain an understanding of how to optimize the recovery of bitumen using petroleum diesel. Finally, the performance of petroleum diesel for extraction of bitumen was investigated at ambient conditions using various experimental techniques.

Additional experiments were conducted using dodecane (key component of petroleum diesel) to compare the performance of bitumen liberation process with that using petroleum diesel. These experiments were designed to help determine whether the natural surfactants of bitumen play a strong role in liberation process of bitumen from ores or not. It also helped to determine if

natural surfactants of petroleum diesel (solvent) play a strong role in liberation process of bitumen from ores.

## **1.5 Thesis Outline**

The thesis is organized into the following sections:

Chapter 1: The general description of current industrial operation for production of bitumen including in-situ and surface mining methods is discussed. The current challenges, which lead to motivation of this thesis, are emphasized here. Last, the key research objectives are discussed in this chapter.

Chapter 2: The characteristics of ores and key process parameters of the extraction process are introduced. The key literature reviews focused on colloids and interface science and fundamentals of bitumen extraction including the bitumen liberation and aeration sub-processes are discussed here. The background of petroleum diesel and other chemical process aids used in the past research work are also discussed.

Chapter 3: Materials including three ores (various grades and fines contents) and petroleum diesel are described. The general descriptions of equipment and experimental protocols are discussed. Various analytical techniques to determine the characteristics of petroleum diesel and several key experiments including the batch extractor (Denver cell) are used to achieve the objectives of the thesis.

Chapter 4: The characterization of petroleum diesel is discussed including the experimental results from analytical techniques. The working mechanism of petroleum diesel when used as a solvent is discussed.

Chapter 5: The performance of petroleum diesel for the hybrid bitumen extraction process is discussed. The effect of petroleum diesel on bitumen liberation and aeration subprocesses is also examined.

Chapter 6: The loss of petroleum diesel to tailings is discussed including the objective, method of solvent loss analysis, results, and conclusion. The reason for why dodecane is used instead of petroleum diesel for solvent loss to tailings analysis is discussed.

Chapter 7: The conclusions from the thesis research to address the objectives are drawn based on experimental results. The key research work is discussed in this section. Finally, the evaluation of petroleum diesel as a solvent for aqueous-nonaqueous extraction process of bitumen from ores is discussed.

Chapter 8: The key contributions to the research work are discussed. A new experimental technique is discussed to provide valuable information for future research work.

Chapter 9: Future research work is discussed based on recommendations from key conclusions and the experimental results. The ideas and suggestions for additional research work are identified which need to be addressed before the concept of aqueous-nonaqueous hybrid extraction process of bitumen from ores can be applied commercially at the site.

## **Chapter 2: Literature Review**

### **2.1 Characterization of Ores**

Petroleum, including bitumen, is a mixture of hydrocarbons with small traces of non-hydrocarbon compounds (~97.5 wt.% of elemental C and H and ~2.5 wt.% of elemental sulfur, oxygen, nitrogen, and metals).<sup>21</sup> The common hydrocarbon groups of petroleum are alkanes, cycloalkanes, aromatics, and naphthenoaromatics. Bitumen typically is a mixture of saturates, aromatics, and heavier components, including resins and asphaltenes.<sup>22</sup> The viscosity of bitumen is extremely high, around  $10^5$ - $10^6$  mPa.s at ambient conditions (25 °C), which can be recovered from oil sands by variety of extraction techniques such as hot-water based extraction, cyclic steam stimulation, steam-assisted gravity drainage, and vapour extraction processes. Saturates and aromatic compounds are easily dissolved in paraffin solvents such as n-heptane whereas asphaltenes are dissolved in aromatic solvents such as toluene.<sup>23</sup> The interfacial tension, which affects the extraction process of bitumen from ores, is influenced by the polar and nonpolar fractions of bitumen.<sup>22</sup> Bitumen contains natural surfactants, mainly carboxylic acids, and sulphonic acids to a small extent, which are beneficial for the extraction process of bitumen from ores.<sup>24</sup>

### **2.2 Key Process Parameters**

There are various parameters of the extraction process that affect bitumen recovery. The high grade (bitumen content) of ores increases the bitumen recovery due to a higher amount of natural surfactants, which decrease the interfacial tension between bitumen and water. There is also an inverse correlation between bitumen recovery and the fines content of ores where the overall recovery of bitumen decreases as the fines content of the ore increases.

Schramm et. al. discovered that viscosity of bitumen is a significant factor in reducing bitumen recovery at 25 °C compared to 50 or 80 °C.<sup>25</sup> However, the overall recovery of bitumen at 25 °C improved significantly when 20,000 ppm of kerosene was dissolved in bitumen during the extraction process, resulting in a significant reduction in bitumen viscosity from ~900,000 mPa.s to ~2,270 mPa.s with the kerosene addition. Schramm et al. has proposed that the threshold of bitumen viscosity for optimal recovery was between 2,270 and 4,690 mPa.s.<sup>25</sup> Note that the viscosity of bitumen is also significantly reduced as temperature increases without diluent addition.

The presence of divalent cations such as calcium and magnesium ions in process water affects the bitumen recovery, especially in the presence of fines due to a slime coating phenomenon shown in Figure 2.1.<sup>26</sup> Here the calcium ion acts as a binder between naphthenic acid and fine solids, which makes bitumen more hydrophilic and makes attachment between bitumen and air bubbles more difficult. The presence of fines and calcium ions in process water significantly increases the induction time for bitumen and air bubble attachment at 25 °C as shown in Figure 2.2, which leads to poor overall bitumen recovery.<sup>26</sup> The weathering of the ores also leads to reduction in bitumen recovery due to increased hydrophobicity of solids over time.<sup>27</sup>

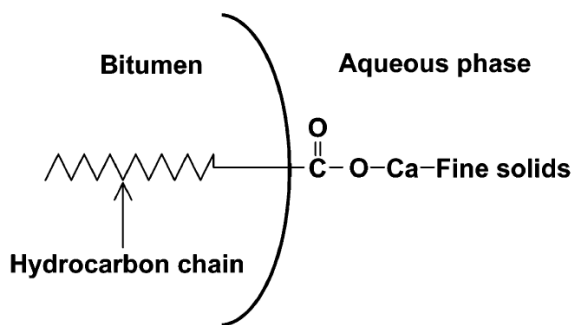


Figure 2.1: Schematic diagram of the calcium binder between bitumen and fines solids.<sup>26</sup>

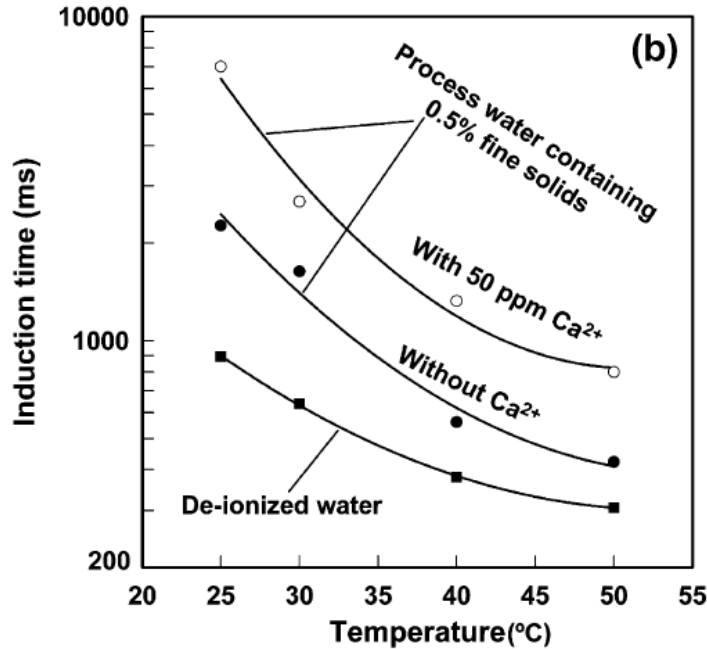


Figure 2.2: Effect of temperature on induction time for air bubble-bitumen attachment.<sup>26</sup>

## 2.2 Interfacial Phenomena

Interfacial energy or interfacial tension is the cost of energy for increasing the unit area of the interface when molecules transfer from bulk phase to the interface of two different phases. The equation for interfacial tension ( $\gamma$ ) at constant temperature ( $T$ ) and pressure ( $P$ ) is:

$$\gamma = \left( \frac{dG}{dA} \right)_{T,P} \quad (2-1)$$

where  $G$  is the Gibbs free energy and  $A$  is the area of the interface.<sup>3</sup> Surface tension is measured between one phase and air. Surface and interfacial tension are measured by a variety of techniques such as spinning drop, sessile drop, and pendant drop methods.<sup>3</sup> The Gibbs equation describes the relationship between interfacial tension and bulk concentration of surfactants ( $C$ ) to

calculate excess concentration of surfactants ( $\Gamma$ ) at the interface, where  $R$  is the universal gas constant:

$$\Gamma = -\frac{1}{RT} \left( \frac{d\gamma}{d \ln C} \right)_P \quad (2-2)$$

The interfacial tension no longer changes when there is maximum concentration of surfactants at the interface that propel surfactants to form micelles in the bulk phase. Bitumen recovery is influenced by interfacial tension between bitumen and water, which changes with temperature and chemical additives dosages.<sup>3</sup>

Emulsions are droplets that are dispersed through the immiscible phase and typically have diameters in the range of 1-10  $\mu\text{m}$ .<sup>24</sup> Asphaltenes, resins, and natural surfactants contribute to the stability of emulsified water (W) droplets in oil (O). The stability of water in oil (W/O) emulsions is required to be low to allow phase separation of water and solids from bitumen to meet the pipeline specification for solids and water contents in crude bitumen.<sup>11</sup> Stable emulsions are not desired in oil sands industries since emulsions contribute to damages in equipment and increases in transportation costs. A novel demulsifier, ethyl cellulose, overcomes this issue by breaking the interfacial film between emulsified water and continuous oil through flocculation and coalescence of phases to accelerate the demulsification process.<sup>28</sup>

## 2.3 Colloids

Colloidal forces play an important role in the oil sands industries. The size of particles ranges from nanometre to micrometre and their interactions involve various attractive and repulsive forces.<sup>29</sup> The electrical double layer (EDL) force is typically a repulsive force between two similarly charged particles in an electrolyte solution and a Van der Waals forces (VDW) are



often attractive between particles. Electrical double layer and Van der Waals forces play a crucial role in colloidal systems. The energy of interaction between two charged particles is described by DLVO theory, developed by Derjaguin, Landau, Verwey, and Overbeek, in equation 2-3<sup>29</sup>:

$$W_{DLVO} = W_{EDL} + W_{VDW} \quad (2-3)$$

Figure 2.3 shows an example of the effect of a monovalent salt concentration on normalized Gibbs free energy,  $W$  ( $k_B T$ ), including electrical double layer and Van der Waal interactions between two identical spheres. As the concentration of salt increases, the electrical double layer repulsive force decreases; therefore the normalized Gibbs free energy of interaction becomes more negative due to compression of the double layer.

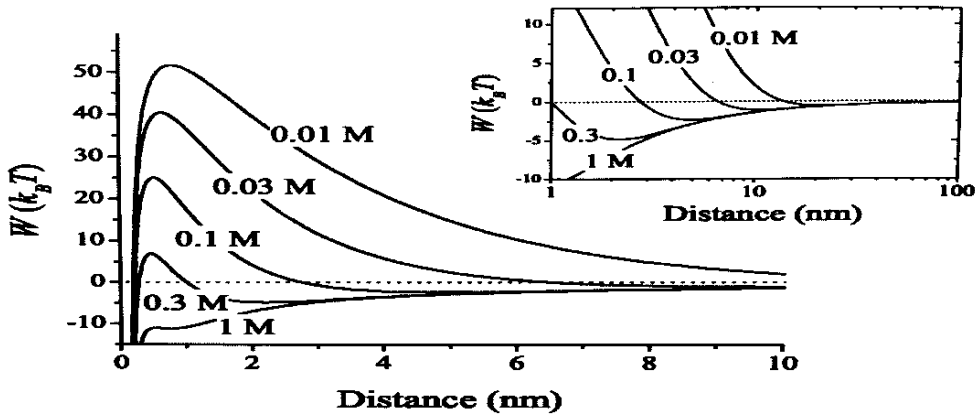


Figure 2.3: Normalized Gibbs free energy of particle interactions versus distance for two identical spherical particles with radius of 100 nm in water, containing different concentration of monovalent salt. The calculation is based on classical DLVO theory. The Hamaker constant was  $7 \times 10^{-21}$  J and the surface potential was 30 mV. The insert picture shows the weak attractive interaction (secondary energy minimum) at very large distances.<sup>30</sup>

There are other forces that play a role in the colloidal system such as hydrophobic force ( $F_{HB}$ ), steric force ( $F_S$ ), and hydration force ( $F_{HD}$ ), that leads to an extended DLVO theory<sup>31</sup>:

$$F_{total} = F_{EDL} + F_{VDW} + F_{HB} + F_S + F_{HD} \quad (2-4)$$

This extended DLVO theory was developed based on deviation of experimental data using atomic force microscopy techniques when classical DLVO theory was used. The increase in salt concentration facilitates coagulation of fines solids and bitumen due to compression of the double layer, which leads to an increased attractive force between bitumen and mineral solids.<sup>31</sup>

The electric double layer force dominates over van der Waal force when the pH of the solution increases; this is due to increased charge density and dissociation of the surface active groups on the bitumen surface. The caustic soda (sodium hydroxide)/pH of the solution play a crucial role in controlling the stability of colloidal systems hence the overall bitumen recovery during the extraction process. The increase in concentration of the calcium ions increases the adhesive force between bitumen and silica, which facilitates the aggregation process or hinders bitumen liberation.<sup>32</sup>

Figure 2.4 shows the schematic diagram of the Guoy-Chapman-Stern model for a charged particle. The surface potential ( $\Psi_0$ ) is located on the surface of the particle and decreases linearly with distance until the stern layer, where the potential is defined as ( $\Psi_\zeta$ ). The potential of the particle decreases exponentially with distance after the stern layer. The surface potential of the particle is not easy to measure; however zeta potential ( $\zeta$ ) of the particle at the slipping shear plane location is easily measured using an electrophoresis technique.<sup>33</sup> Zeta potential describes the stability of emulsions and particles in a colloidal system. In the electrophoresis technique, the velocity of particles under an electric field is known as electrophoretic mobility, which converts

to the zeta potential using the following Helmholtz-Smoluchowski (HS) equation for particles of diameters  $\geq 1 \mu\text{m}$  and ionic strengths  $\geq 1\text{mM}$ :

$$\zeta = \frac{\mu U_E}{\varepsilon} \quad (2-5)$$

where  $\mu$  is the aqueous viscosity,  $\varepsilon$  is the dielectric constant of aqueous solution,  $U_E$  is electrophoretic mobility of the particle.<sup>33</sup>

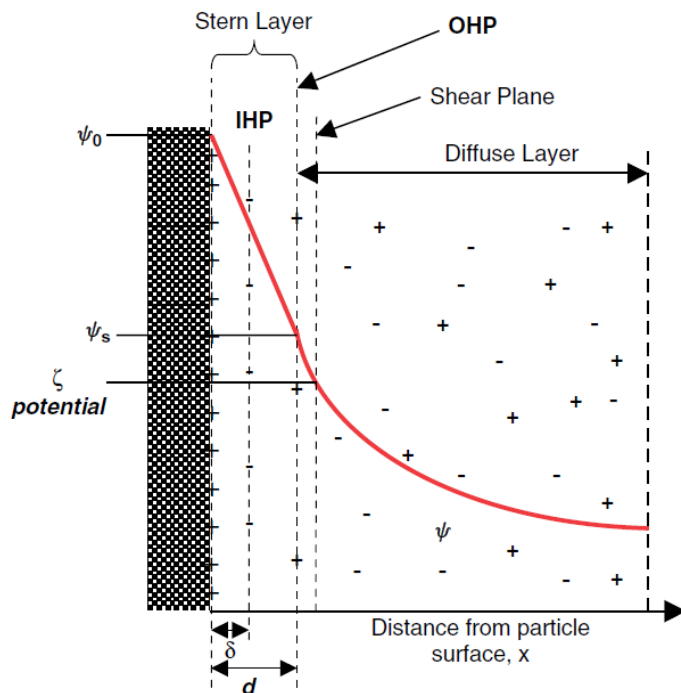


Figure 2.4: Typical diagram of Gouy-Chapman-Stern model.<sup>29</sup>

## 2.4 Extraction Sub-Processes

There are two key sub-processes of the extraction process: the liberation process and the aeration process. The liberation process involves thinning of the bitumen film, followed by separation of the bitumen from the ores. The aeration process involves the rupture of the water film to

facilitate attachment between bitumen and air bubbles. The scientific explanations for the sub-processes are described below:

### **2.4.1 Liberation Process**

Wang et al. proposed the main stages of the bitumen liberation as the following: the thinning of the bitumen film and rupture, the replacement of the solid/bitumen interface with a solid/water interface, leading to the formation of bitumen droplets, and the detachment of the bitumen droplets from the solid surface.<sup>34</sup> Also, Wang et. al. studied the effect of diluents (kerosene and fatty acid methyl ester) on the liberation of bitumen from a glass surface. They found that the degree of bitumen liberation (%) improved as the dosage and temperature increased for both cases of kerosene and fatty acid methyl ester. Based on rheological studies, the main contribution to the improvement in the liberation of bitumen from the hydrophilic surface is due to the reduced bitumen viscosity.<sup>34</sup> He et al. proposed that toluene and naphtha, acting as solvents, lead to significant reduction in interfacial tension and viscosity of bitumen in an aqueous environment, which improves the degree of bitumen liberation due to the enhanced transportation of bitumen natural surfactants to the bitumen-water interface.<sup>35</sup>

The change in interfacial tensions between bitumen (B), water (W), and mineral solids (S) contribute to the improvement in bitumen liberation as demonstrated by the Young's equation:

$$\gamma_{B/S} - \gamma_{S/W} = \gamma_{B/W} \cos \theta \quad (2-6)$$

where  $\theta$  is measured through the aqueous phase.<sup>16</sup> The increase in pH leads to deprotonation of natural surfactants (mainly carboxylic acid groups, R-COOH), which initiates the migration from

bulk bitumen to the interface and hydrolysis of the solids surface, which makes the solids surface more hydrophilic. Figure 2.5 shows the interfacial tension (force) balance of a B/W/S system.

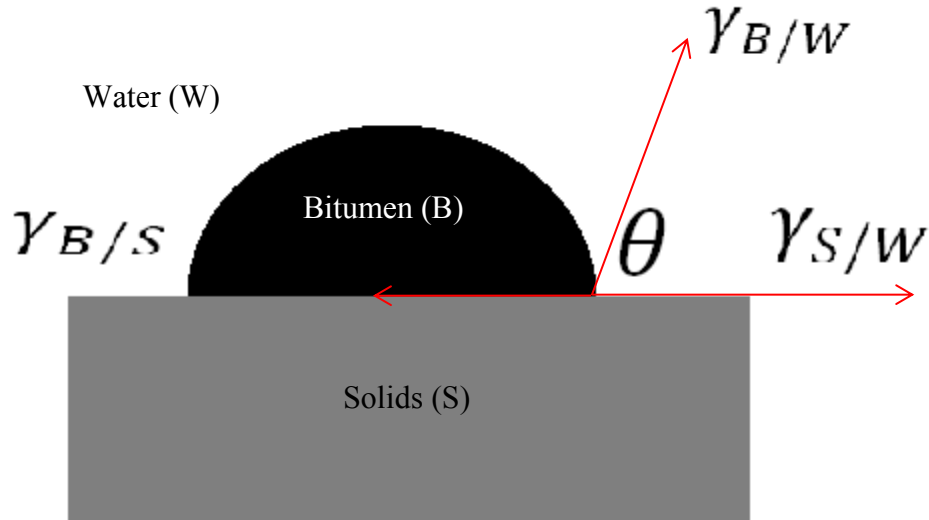
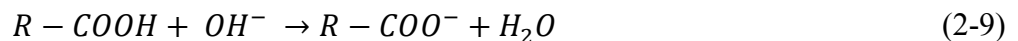


Figure 2.5: Schematic diagram of a bitumen droplet on solids in water.

The increase in pH leads to lower interfacial tension between bitumen and water and the interfacial tension between water and solids.<sup>16</sup> As a result, the contact angle ( $\theta$ ) is lower and thermodynamically favours the thinning of the bitumen film as seen by Wang et. al.<sup>34</sup> Equations (2-7) to (2-9) show the key mechanisms of the bitumen liberation process.<sup>16</sup> The key mechanisms below show that there is a repulsion between silica sand and bitumen, which enhance the liberation of bitumen upon addition of sodium hydroxide.



### 2.4.2 Aeration Process

The aeration process is the key sub-process of bitumen extraction. The aeration process occurs in hydrotransport pipelines, primary separation vessels, and secondary flotation units, and involves attachment of bitumen to air bubbles under hydrodynamic conditions. This results in a lower apparent density than the aqueous solution and floats the bitumen to the surface in the froth layer.<sup>16</sup> The key equation that describes bitumen and air (*A*) bubble attachment in water (*W*) is given by<sup>16</sup>:

$$\frac{\Delta G}{\Delta A} = \gamma_{A/W}(\cos \theta - 1) \quad (2-10)$$

The attachment between bitumen and air bubbles occurs spontaneously when  $\theta > 0$  since  $\frac{\Delta G}{\Delta A}$  is less than zero due to the hydrophobicity of bitumen, which prefers to be attached to an air bubble in an aqueous environment. Figure 2.6 shows the common diagram of bitumen and air bubble attachment.<sup>36</sup> Bitumen is able to spread easily around the air bubble when the temperature of the process water increases, leading to an increased aeration efficiency. However, the increase in pH leads to poorer performance of bitumen and air bubble attachment due to an increase in ionization of naphthenic acid groups in bitumen.<sup>16</sup> Lower pH is favorable for aeration process of bitumen under a given hydrodynamic condition.<sup>16</sup>

There is a thin aqueous film between bitumen and air bubbles. Induction time is the key parameter that describes the performance of bitumen and air bubble attachment. Induction time is the minimum time required for thinning of water film to a critical thickness at which the film ruptures spontaneously before the attachment between bitumen and air bubble occurs.<sup>37</sup> He et. al. proposed an optimal solvent (toluene and naphtha) addition at 10 wt.% to achieve the minimum induction time for bitumen and air bubble attachment based on experimental data.<sup>37</sup>

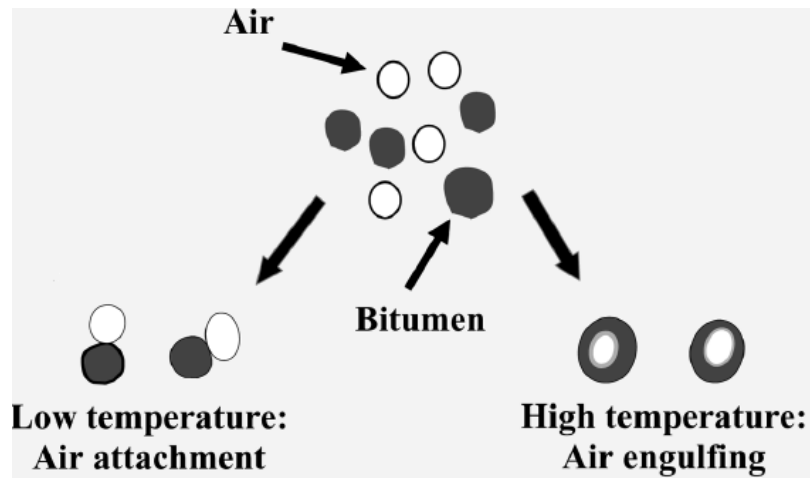


Figure 2.6: Schematic diagram of aeration process of bitumen.<sup>36</sup>

## 2.5 Chemical Process Aids

There are various chemical process aids that were studied in the past to improve the extraction of bitumen from ores. Schramm et al. found out that kerosene and a mixture of kerosene and methylisobutyl carbinol (MIBC) increased bitumen recovery at ambient condition (25 °C) mainly due to the lower bitumen viscosity.<sup>25</sup> It was observed that the dynamic degree of bitumen liberation improved as ethyl cellulose and ethylene oxide/propylene oxide (demulsifiers) were added to heavy oil around host rocks, leading to improved efficiency of unconventional oils extraction processes.<sup>38</sup> Demulsifiers contains hydrophilic and hydrophobic groups, which lead to the reduction in interfacial tensions between bitumen and water and hence improves the bitumen liberation process. The chemical process aids improve bitumen recovery mainly due to improved liberation process of bitumen from mineral solids or host rocks.

Some solvents have been studied in the past to evaluate the novel concept of an aqueous-nonaqueous hybrid bitumen extraction process. Harjai et. al. studied the concept of using kerosene, which is one of by-products from crude bitumen, and it was successful in increasing

bitumen recovery as the kerosene dosages increased even at 35 °C and a current operating pH of 8.5.<sup>19</sup> He et al. investigated the effects of toluene and naphtha on liberation of bitumen from ores at ambient condition (20 °C) and they found that use of these solvents improved the degree of bitumen liberation.<sup>35</sup> All of these solvents lead to the reduction in viscosity of bitumen.

While these solvents seem promising for the aqueous-nonaqueous hybrid bitumen extraction, it is not applied commercially due to its toxicity, health, or volatility concerns. This gives a motivation that petroleum diesel may work better as a solvent for aqueous-nonaqueous hybrid bitumen extraction process since it is less volatile under ambient condition and is a by-product of crude bitumen, which can potentially lower operating costs relative to the use of external chemical additives.

## **2.6 Petroleum Diesel**

Petroleum diesel is a mixture of hydrocarbon compounds including aliphatic and aromatic compounds. Petroleum diesel is one of key products that is produced during the distillation process of crude bitumen and is widely used as fuel for variety of vehicles including cars, marine vessels, buses, and farm equipments.<sup>39</sup> More recently, environmental regulations were created to restrict the sulfur content of petroleum diesel fuel to 10-15 ppm (to prevent accumulation of SO<sub>x</sub> compounds) and to improve (lower) the formation of harmful compounds such as carbon monoxide and volatile organic matter.

The density of petroleum diesel typically varies between 819 and 841 kg/m<sup>3</sup> and majority of petroleum diesel is produced during the distillation process at 350 °C.<sup>40</sup> Typically there is also a small trace of sulfur in petroleum diesel, which can vary from 4 to 245 ppm. Petroleum diesel contains paraffin-naphthalene hydrocarbon compounds and n-alkanes with C<sub>9</sub>-C<sub>24</sub> in the



hydrocarbon chains.<sup>40</sup> The cetane number is a key parameter that describes the performance of petroleum diesel fuel for ignition quality. Petroleum diesel with higher cetane number reduces exhaust smoking and hazardous emissions through effective combustion of the mixture.<sup>40</sup> The hydrocarbon composition of petroleum diesel affects the performance of petroleum diesel use as a fuel and for other applications.

The petroleum diesel fraction of the petroleum distillates is one of main raw materials for production of naphthenic acids.<sup>41</sup> Naphthenic acid contains complex mixtures of carboxylic acids with the general formula, RCOOH where R represents naphthene containing cyclopentane and cyclohexane derivatives.<sup>21,41</sup> The carboxylic acid contains the surface active group (-COOH), which is hydrophilic and thermodynamically favours to be at the aqueous phase resulting in lower interfacial tension. Figure 2.7 shows a simple schematic diagram of the common natural surfactant in petroleum diesel and bitumen. It is evident that petroleum diesel may contain naphthenic acid and sulfonic acid since petroleum diesel is a by-product of bitumen, which has the same kind of natural surfactants.

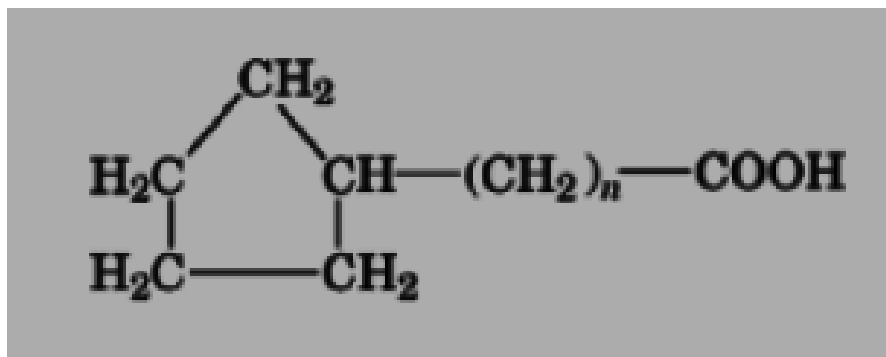


Figure 2.7: Simple model of naphthenic acid.<sup>41</sup>

## Chapter 3: Research Methodology

### 3.1 Petroleum Diesel (Commercial Fuel)

Table 3.1 shows the specifications of a commercial petroleum diesel fuel that was obtained from a Shell Canada gasoline station (in Edmonton), for this thesis project. The diesel fuel was reported to have  $\leq 15$  ppm of elemental sulfur and a total acid number of 100 mg KOH/kg (100 ppm). The density of petroleum diesel was found to be 841 kg/m<sup>3</sup> based on density laboratory measurement. The maximum viscosity of petroleum diesel was 3.03 mPa.s at 40 °C. Commercial petroleum diesel fuel can contain up to 5% biodiesel by volume.

Table 3.1: Specifications of petroleum diesel used in thesis project (Shell Canada).

Product Name:	<b>TYPE B - ULTRA LOW SULPHUR DIESEL FUEL</b> <b>TYPE B – DIESEL FUEL</b> (MAY BE DYED OR UNDYED FOR TAX PURPOSES)	Issued: <u>30-July-2015</u>
Page 1 of 1		Cancels: <u>20-Aug-2013</u>

**◆ SPECIFICATION ◆**

Spec Characteristic	Units	ASTM Method	Minimum	Maximum
Appearance		D4176 – Proc. 1	Clear & Bright	
Ash	% by mass	D482		0.010
Cetane Number		D613	40.0	
Cloud Point	°C	D5773	Seasonal <sup>1</sup>	
Conductivity	pS/m	D2624	25 <sup>2</sup>	
Copper Strip Corrosion, 3 h at min 50 °C		D130		No. 1
Distillation 90 % recovered	°C	D86		360.0
Flash	°C	D93	40.0	
Lubricity			Satisfactory <sup>3</sup>	
Carbon Residue on 10% bottoms	% by mass	D4530		0.2
Sulphur	mg/kg	D5453		15
Total Acid No.	mg KOH/g	D974		0.10
Viscosity at 40 °C	cSt	D445	1.70 <sup>4</sup>	3.60
Water & Sediment	% by volume	D1796-Mod. or D2709		0.02

**◆ COMMENTS ◆**

Approval Comments
<p>Meets: The latest edition and amendment of CAN/CGSB-3.517 "Diesel Fuel" Type B when supplied to meet the 2.5 % low-end design temperature for the period and location of intended use.</p> <p>May contain up to 5% by volume Biodiesel (FAME or Fatty Acid Methyl Esters) when the 2.5% low-end design temperature is warmer than -18°C.</p> <p>If the fuel contains over 1.0% by volume biodiesel then the product meets the latest edition and amendment of CAN/CGSB-3.520 "Automotive Diesel Fuel containing Low Levels of Biodiesel (B1-B5)" Type B.</p> <p>The latest edition and amendment of CAN/CGSB-3.2 "Heating Oil" Type 2</p>

### 3.2 Characterization of Oil Sands Ores

Three different types of oil sands ores were used in thesis research project. Table 3.2 shows the key composition of the oil sands ores. Bitumen and fines compositions of the ores were obtained by Rui Lu and from Syncrude as these ores were used for other studies. The fines are defined as the percentage of mineral solids with particle size less than 44  $\mu\text{m}$ . All samples were kept in the freezer to avoid oxidation. The samples were allowed to thaw overnight in a tight bag prior to extraction and bitumen liberation experiments. All oil sands ores in Table 3.2 have different bitumen and fines contents, which provide useful analysis in effects of oil sands ore characteristics on overall recovery of bitumen during the bitumen extraction process of oil sands ores.

Table 3.2: Composition of oil sands ores used for the study.

Oil Sands Ores	Bitumen (wt.%)	Water (wt.%)*	Solids (wt.%)*	Fines (wt.%)
AK (2015)	9.20	5.25	85.51	43
AD (2015)	10.00	4.21	85.80	21
AC (2016)	11.40	3.23**	84.86**	22

\* Determined experimentally using Dean Stark extraction method

\*\* Average values based on two samples

### 3.3 Extraction Process Water and Mineralogy of Fines

Process water was provided by Syncrude Canada (Aurora mine site) with natural pH of  $7.52 \pm 0.05$ . The pH of the process water was adjusted to the desired values by hydrochloric acid and sodium hydroxide (obtained from Fisher Scientific). The ion composition of the process water was analyzed (courtesy of Jie Ru and Yi Lu) using an ion chromatography instrument (Dionex

ICS-3000). The ion compositions of the process water are given in Table 3.3. All the numbers in Table 3.3 are similar to the results obtained in previous research work.<sup>19</sup>

Table 3.3: Composition of Aurora process water determined by ion chromatography.

<b>Ions</b>	<b>Concentration (ppm)</b>
Na <sup>+</sup>	691
K <sup>+</sup>	21
Mg <sup>2+</sup>	19
Ca <sup>2+</sup>	83
Cl <sup>-</sup>	444

Fine particles (#BHF0073P2) from an oil sand deposit were provided by Teck Limited to investigate the effect of fines on induction time for bitumen-air bubble attachment. The mineral composition of the fines analyzed using x-ray diffraction techniques is given in Table 3.4.

Table 3.4: Mineralogy composition of fine particles by x-ray diffraction.

<b>Composition</b>	<b>Bulk Fraction (wt%)</b>	<b>Clay Fraction (wt%)</b>	<b>Overall (wt%)</b>
All Solids	59.86 ± 6.63	40.14 ± 6.63	100 ± 0.00
Total Clay	19.40 ± 5.47	88.97 ± 5.41	47.33 ± 1.08
Quartz	77.00 ± 5.67	11.03 ± 5.41	50.51 ± 1.26
K-feldspar	1.14 ± 0.81	-	0.67 ± 0.43
Plagioclase	0.41 ± 0.08	-	0.25 ± 0.08
Calcite	0.54 ± 0.20	-	0.33 ± 0.16
Dolomite	0.31 ± 0.12	-	0.19 ± 0.10
Siderite	0.73 ± 0.13	-	0.44 ± 0.09
Pyrite	0.46 ± 0.29	-	0.29 ± 0.22
Chlorite	0.75 ± 0.05	2.45 ± 0.28	1.42 ± 0.04
Kaolinite	6.02 ± 1.81	46.30 ± 2.81	22.22 ± 1.51
Illite	12.63 ± 3.76	38.64 ± 4.65	23.05 ± 2.07
Illite/Smectite Mixed Layer	0.00 ± 0.00	1.58 ± 0.27	0.64 ± 0.19

## **3.2 Experimental Methods**

### **3.3.1 Gas Chromatography/Mass Spectrometry (GC-MS)**

Thermo Gravimetric Analysis (TGA) equipment was used to monitor the change in mass of the petroleum diesel sample over time at a constant heating rate of 15.0 °C/min. The initial temperature of the petroleum diesel sample was set at ~27°C and the final temperature was at ~457 °C. Nitrogen purge gas was set at 25 mL/min throughout the experiment. A small sample of petroleum diesel (~16.5 mg) was used for the TGA experiments. The evaporated petroleum diesel gas was transferred to a Gas Chromatography-Mass Spectrometer (manufactured by Agilent Technologies) to identify the composition of the petroleum diesel sample. Liquid carbon dioxide was used to trap the sample at about -35 °C.

### **3.3.2 Fourier Transform Infrared Spectroscopy**

A Fourier Transform Infrared Spectroscopy (FTIR) unit (Thermo Scientific iS50 FT-IR model) was used [in the Attenuated Total Reflection (ATR) method] to obtain infrared spectra of petroleum diesel that allows identification of the key functional groups of petroleum diesel. A small drop of petroleum diesel was used to obtain the spectral data over a wavenumber range between 650 cm<sup>-1</sup> and 4000 cm<sup>-1</sup>. Air was used as background for each spectral experiment of the petroleum diesel sample. The spectral resolution was set at 4 cm<sup>-1</sup> and 32 scans of spectra were collected during the measurement.

### **3.2.3 Tensiometry**

The Kruss K12 tensiometer was used to measure the surface tension and interfacial tension between petroleum diesel and deionized water (resistivity of 18.2 MΩ cm) at various pH levels employing the Du Nouy ring method. All experiments were conducted at a temperature of 21.5 ±

0.5 °C. Figure 3.1 shows the schematic diagram of the tensiometer used for measuring interfacial tension between lighter phase (petroleum diesel) and heavier phase (deionized water). The net force between total force ( $F_{tot}$ ) and gravitational force ( $G_{ring}$ ) is due to interfacial tension ( $\gamma$ ) at the interface between two immiscible phases. The interfacial tension is calculated using equation 3-1 where  $R$  is the radius of the Du Nouy ring.

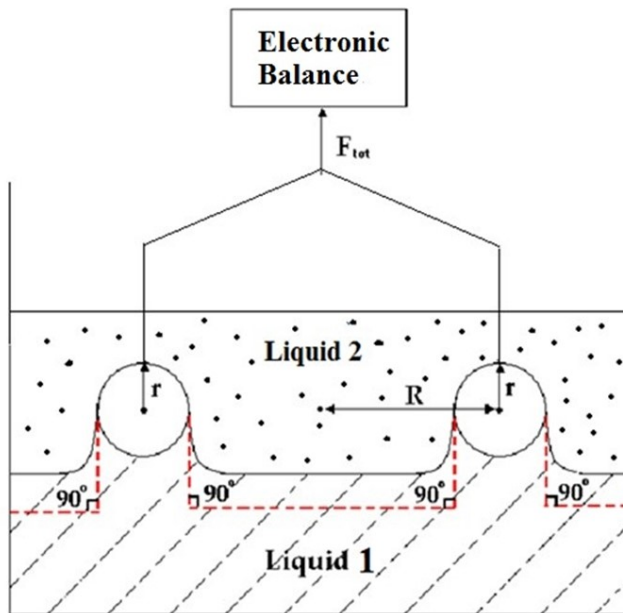


Figure 3.1: Schematic diagram of the tensiometer (Du Nouy ring).

$$\gamma = \frac{F_{tot} - G_{ring}}{4\pi R} \quad (3-1)$$

### 3.2.4 Electrophoresis

A Homogenizer (VWR 250 model) was used to homogenize the electrolyte stock solution (10 mM potassium chloride) containing 5 wt.% of petroleum diesel at 10,000 rpm for five minutes. This equipment applied high shear rate to form stable petroleum diesel in water emulsions with an average particle size range of 2.5 – 6  $\mu\text{m}$  that was suitable for zeta potential measurements using the Zetasizer Nano instrument (Malvern).<sup>42</sup> The Zetasizer Nano instrument using a red

laser (633 nm) was applied to the emulsified petroleum diesel in 10 mM potassium chloride (KCl) solution at different pH levels. The principles of electrophoresis and laser doppler velocimetry were used to obtain electrophoretic mobility of the emulsified petroleum diesel. The electrophoretic mobility of emulsified petroleum diesel was then converted to zeta potential using the Smoluchowski equation (equation 2-5).

A 200  $\mu$ L sample of the stock solution was transferred to 20 mL of the electrolyte solution at a specific pH. Ultrasonication of the final solution for 15 minutes was necessary to remove bubbles and to ensure that emulsified petroleum diesel droplets were stable prior to the zeta potential measurement. The viscosity and dielectric constant values of water were used for all calculations. The refractive index (1.47) and absorbance (0.01) of petroleum diesel were used in the software to obtain the measured zeta potential of emulsified petroleum diesel in the electrolyte solution. The refractive index (1.47) of petroleum diesel was obtained using the near infrared spectroscopy and Terahertz Time Domain Spectroscopy techniques in the previous work.<sup>43,44</sup> A total of 6 runs were conducted for each experiment. Each experiment was repeated several times for each sample from the final emulsion to obtain an averaged zeta potential value at a specific pH. All experiments were conducted at 25 °C.

### **3.3.5 Batch Extraction Test Procedure**

A batch extractor (Denver flotation cell) was used to determine the overall hydrocarbon recovery of oil sands ores (bitumen and petroleum diesel combined) during the flotation process at various petroleum diesel dosages. The temperature of the ores and water slurry mixture was controlled by the circulation of water flowing inside the cell from a water bath. The temperature and pH of the Aurora process water were set at  $25 \pm 0.5$  °C and  $7.52 \pm 0.05$ , respectively. A  $500 \pm 0.5$  g sample of ore was used for each flotation experiment. The ores were soaked with petroleum

diesel for 15 minutes in a glass pan. The petroleum diesel dosage used (wt.%) was with respect to bitumen content of the ores. There was negligible change in total mass of the oil sands ores and petroleum diesel (< 0.1 wt.%) after 15 minutes of the soaking process. This confirmed that petroleum diesel was stable and did not evaporate at room temperature. A 250 g sample of the process water was added to the flotation cell containing the pretreated ores. The conditioning stage of the flotation experiment took place at an impeller speed of 600 rpm and an air flow rate of 150 mL/min for 10 minutes. After this, another 800 g of process water was added to the slurry while the impeller was rotating for 10 minutes at the same operating conditions. This stage is known as primary flotation process.

The froth from the experiment was collected into a thimble using a spatula during the last five minutes of the primary flotation process. The speed of impeller was then increased to 800 rpm for 10 minutes as part of the secondary flotation process to further recover hydrocarbon compounds. The secondary froth was collected into the second thimble during the last five minutes of the secondary flotation process. The schematic diagram of the Denver flotation cell apparatus is shown in Figure 3.2.

A Dean Stark Extraction apparatus was used to determine the hydrocarbon (bitumen and petroleum diesel), water, and solids mass contents of the primary froth and secondary froth. Toluene was used as the refluxing solvent to extract bitumen and petroleum diesel from froth. The temperature was set at 175 – 210 °C during the process. The total hydrocarbon recovery was calculated using equation (3-2).

$$Total\ Hydrocarbon\ Recovery = \left( \frac{m_{bitumen\ and\ diesel\ in\ froth}}{m_{bitumen\ in\ ore} + m_{diesel}} \right) \times 100\% \quad (3-2)$$



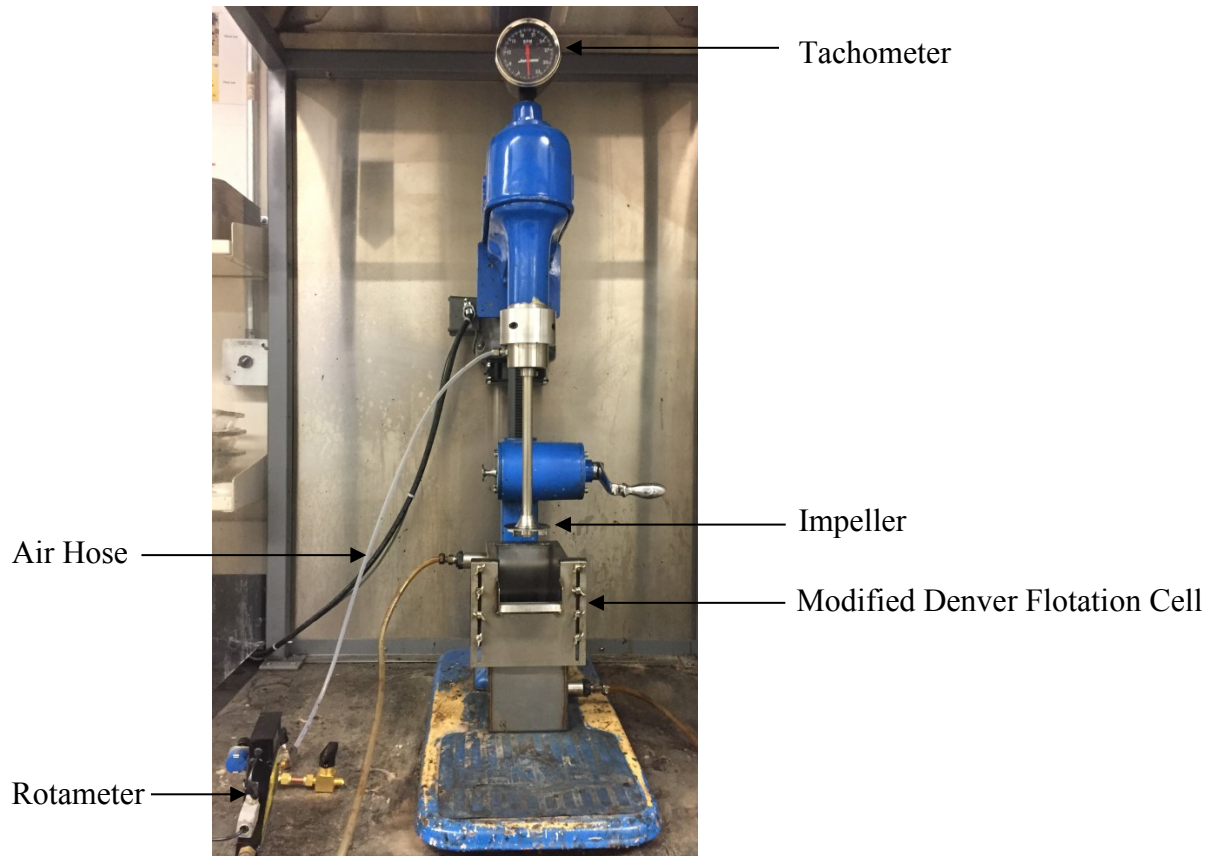


Figure 3.2: Photograph of Denver flotation extraction used in this study.

### 3.3.6 Optical Microscopy

An optical microscope (Olympus SZX10) was used to monitor the liberation process of bitumen from ores in the Aurora process water at a constant temperature of  $25 \pm 0.5$  °C and a pH of  $7.52 \pm 0.05$ . Petroleum diesel was used to penetrate the ores (soaked for 15 minutes) during the pre-treatment process prior to bitumen liberation experiments. The treated ore samples were flattened down on the sample holder using a metal rod. The surface of the sample was then filled with process water. Images were collected immediately during the bitumen liberation process over the next five minutes (~300 s). Figure 3.3 shows the apparatus set up for the imaging acquisition. The experiments were repeated several times for each experimental condition.

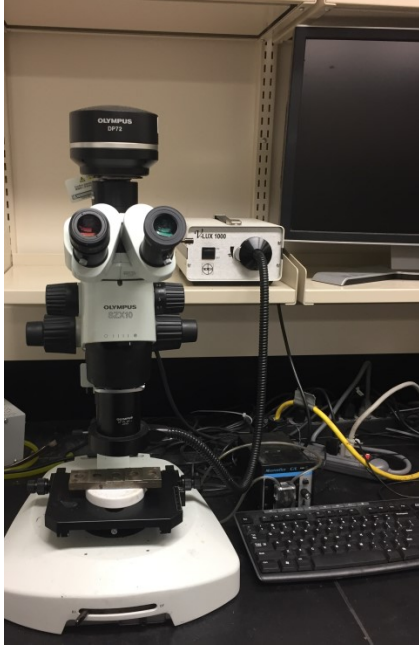


Figure 3.3: Photograph of optical microscope for visualization of bitumen liberation process.

A Modified empirical method was used instead of a more traditional empirical method (greyscale threshold of  $X = 80$ ) for the bitumen liberation data analysis of the experimental run.

The equation for the modified empirical method (3-3) is given below<sup>45</sup>:

$$\text{Threshold Greyscale} = \frac{X_{\text{minimum\_liberated}} + X_{\text{maximum\_unliberated}}}{2} \quad (3-3)$$

The image of the last picture (300s into the liberation process) was converted to greyscale using the MATLAB program. Multiple points of the liberated surface and unliberated surface were selected to calculate the threshold greyscale value using equation 3-2. Once the threshold greyscale value was obtained, the degree of bitumen liberation,  $DBL$  (%), was calculated using equation 3-4 below<sup>45</sup>:

$$DBL (\%) = \frac{N_0 - N_t}{N_0} \times 100\% \quad (3-4)$$

where  $N_0$  is the number of black pixels (below the greyscale threshold number) at time zero and  $N_t$  is the number of black pixels at a certain time. The equation is based on the assumption that there are no black pixels when all bitumen is liberated from the surface. This assumption is valid since the number of black pixels of the cleaned ore samples after the Dean Stark extraction process was close to zero. A first order kinetic model was used for all experimental runs to evaluate the bitumen liberation process performance. The first order kinetic model is given below:

$$DBL (\%) = A_0(1 - e^{-kt}) \quad (3-5)$$

where  $A_0$  can be defined as ultimate bitumen liberation and  $k$  is the rate constant, which is the key parameter that describes the performance of bitumen liberation process.<sup>20</sup> The Origin software was used to calculate the rate constant,  $k$ , for all experiments.

### **3.3.7 Custom Designed Induction Timer Device**

The aeration process of bitumen was studied using a custom designed induction timer device at various petroleum diesel dosages. Vacuum distillation feed bitumen (Syncrude) was used for all induction timer experiments. Petroleum diesel was added to the bitumen sample followed by the mixing process at moderate temperature to achieve homogeneity of the mixture. The sample was added to the teflon plate to obtain an uniform surface after 20 minutes. Then, the sample was transferred to the rectangular glass cell containing the Aurora process water at  $\text{pH } 7.52 \pm 0.05$ . This sample was equilibrated for 30 minutes prior to the induction timer experiment. The

temperature of the process water was set at  $25 \pm 1^\circ\text{C}$ , which was controlled using the portable heater for all experiments. Twenty five trials were conducted at each contact time to obtain a statistical curve. The induction time, which is the contact time at which 50% probability of attachment occurs, was determined through interpolation of experimental data. The diameter of the bubble was set at 1.5 mm. The displacement of the air bubble was set at 0.40 mm and the initial gap between the air bubble and the sample was set at 0.25 mm. The approach and retract speed of the air bubble was both set at 4.0 cm/s. The air bubble was generated using the microsyringe. The apparatus set up of the custom designed induction timer is given in Figure 3.4.

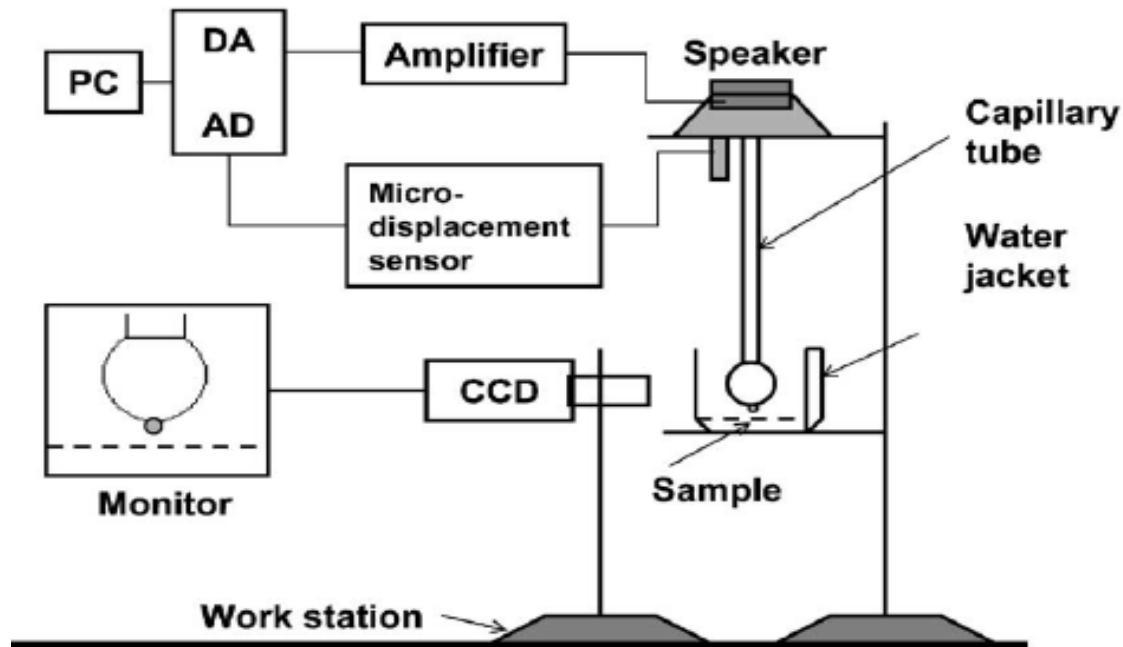


Figure 3.4: Schematics of a custom designed induction timer for aeration experiments.<sup>26</sup>

A procedure developed by Tong Chen was used to prepare the bitumen sample, which was coated with Teck fines particles (#BHF0073P2). The fines particles were ground to  $< 45 \mu\text{m}$  and 0.5 wt.% of fines particles were added to the Aurora process water. The bitumen sample was then inserted upside down into the process water containing 0.5 wt.% fines particles and slowly

stirred by a magnetic stirrer for 15 minutes, prior to the equilibration process and the induction timer experiment. Figure 3.5 shows the apparatus set up for the preparation of a fines-coated bitumen sample.

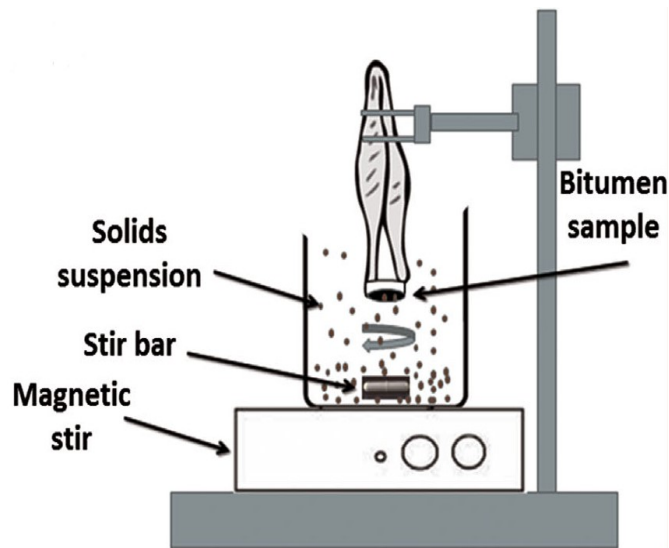


Figure 3.5: Apparatus for preparation of fines-coating on bitumen.<sup>46</sup>

## **Chapter 4: Results and Discussion - Characterization of Petroleum**

### **Diesel**

Various analytical techniques were used to gain a more fundamental understanding of the petroleum diesel used as a solvent for this study. The gas chromatography/mass spectrometry and fourier transform infrared spectroscopy techniques were used to determine the composition of petroleum diesel. Lastly, interfacial tension and zeta potential measurements were conducted to explain the ionization mechanism of surface active species in petroleum diesel.

#### **4.1 Composition of Petroleum Diesel**

Figure 4.1 shows the thermogravimetric curve of the petroleum diesel sample over the temperature range up to 250 °C. The rate of mass loss was maximized at temperature of 161.7 °C. This corresponded to the inflection point of the weight loss curve in Figure 4.1. The differential curve was broad in Figure 4.1, which concludes that petroleum diesel contains many different hydrocarbon compounds that vaporize at certain temperatures. Majority of petroleum diesel components were vaporized at temperature of 225 °C. The final weight of the petroleum diesel sample was about 2.9 % at the final temperature of 456.7 °C. This indicates that there are some leftover compounds in the petroleum diesel, which were not detected by the GC-MS equipment since these compounds did not convert to gas at high temperature (up to 456.7 °C).

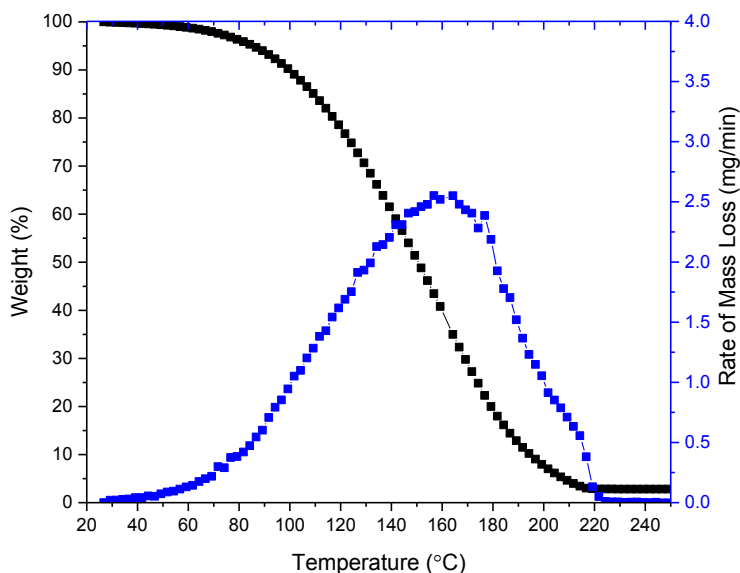


Figure 4.1: Thermogravimetric curve of petroleum diesel.

Figure 4.2 shows the relative abundance of the key components in petroleum diesel with respect to the tallest peak in abundance versus retention time from the GC-MS experiment. The tallest peak corresponded to the presence of undecane in petroleum diesel. It was found from Figure 4.2 that there were 103 different possible compounds in petroleum diesel. Generally, the compounds with the highest abundance in Figure 4.2 had aliphatic and aromatic hydrocarbon groups. Interestingly, petroleum diesel contains aromatic groups such as trans-decahydronaphthalene and benzene. This explains why petroleum diesel is an effective solvent for bitumen extraction since the aromatic groups of petroleum diesel are able to disaggregate the asphaltene molecules, resulting in significant reduction in bitumen viscosity.

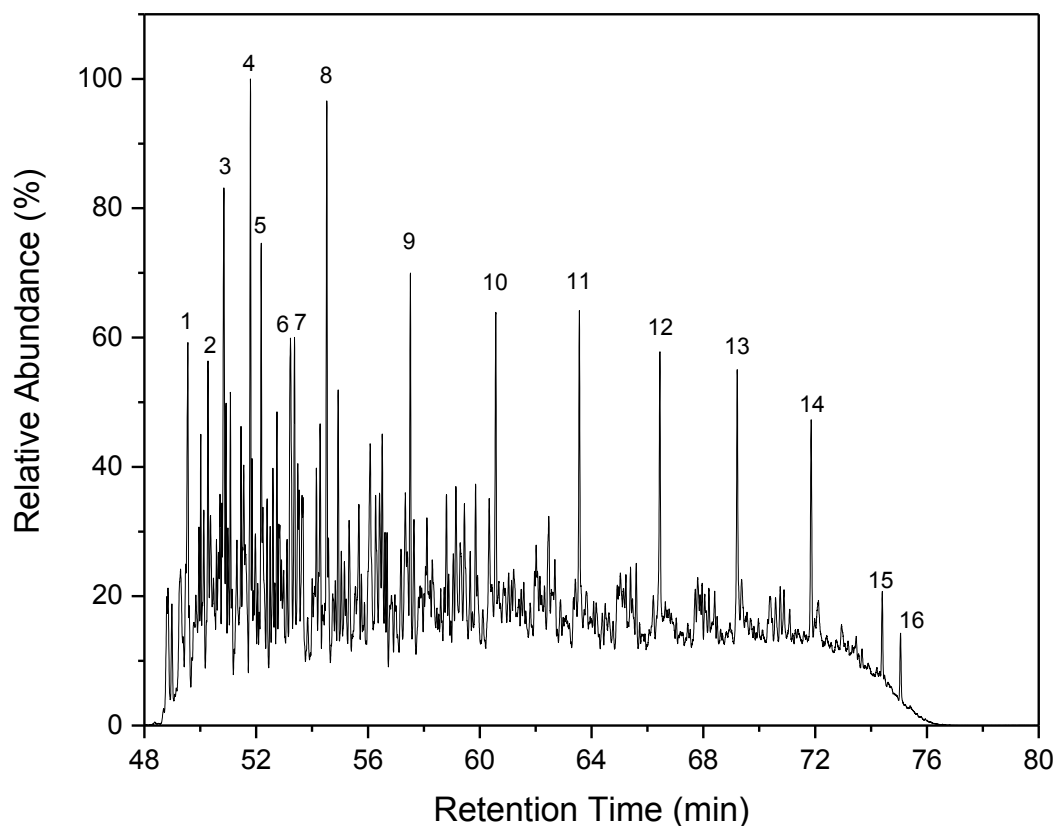


Figure 4.2: Total ion chromatograms for the evaporated petroleum diesel at 500 °C. (1) decane; (2) 2-methylpropyl-cyclohexane; (3) trans-decahydronaphthalene; (4) undecane; (5) 2-methyltransdecalin; (6) 2-phenylpropyl tert.butyl ether; (7) 4-methyl-undecane; (8) dodecane; (9) tridecane; (10) tetradecane; (11) pentadecane; (12) hexadecane; (13) heptadecane; (14) octadecane; (15) hexadecane; (16) hexadecanoic acid, methyl ester.

Table 4.1 shows the compounds of petroleum diesel containing oxygen, nitrogen, and sulphur atoms. The presence of sulfurous acid, ester functional group in the petroleum diesel suggests that the petroleum diesel contains the sulfate, sulfonic acid, and/or sulfone functional groups. The petroleum diesel contained trace of biodiesel compounds as confirmed by the presence of hexadecanoic acid, methyl ester compound (see Figure 4.2). The hexadecanoic acid, methyl ester contains surface active groups (ester and carbonyl functional groups).



Petroleum diesel possibly contains oxalic acid, cyclohexylmethyl isohexyl ester and 6-Octen-1-ol, 3,7-dimethyl-, acetate compounds. These compounds have carbonyl and ester functional groups. It is possible that petroleum diesel contains 1-ethenyl-cyclododecanol, which has the hydroxyl group. The 2-phenylpropyl tert.butyl ether compound contains the ether group, which can be the surface active component of petroleum diesel. However, the experimental result of 2-phenylpropyl tert.butyl ether compound did not match the spectrum library of pure 2-phenylpropyl tert.butyl ether compound well (quality result of 35%). It can be suggested that the carboxylic acid group was attached to various hydrocarbon compounds in the petroleum diesel. Based on the results in Table 4.1, it can be concluded that petroleum diesel contains the carbonyl, ester, and sulfonyl functional groups, which are the common functional groups found in natural surfactants of bitumen.

Table 4.1: Chemical composition of petroleum diesel containing heteroatoms.

Chemical	CAS	Quality of Experimental Data to Spectral Library Result (%)	%Abundance Relative to Undecane Peak
Hexadecanoic acid, methyl ester	000112-39-0	97	14.28
Sulfurous acid, butyl heptadecyl ester	1000309-18-4	87	24.21
Sulfurous acid, butyl heptadecyl ester	1000309-18-4	80	22.89
Oxalic acid, cyclohexylmethyl isohexyl ester	1000309-68-3	72	46.20
Sulfurous acid, butyl undecyl ester	1000309-17-8	72	29.87
Sulfurous acid, butyl tetradecyl ester	1000309-18-1	64	24.58
1-Decanol, 2-hexyl-	002425-77-6	64	27.90
Nonadecyl pentafluoropropionate	1000351-88-8	62	19.85
Sulfurous acid, 2-propyl tetradecyl ester	1000309-12-5	62	21.09
Ether, 2-phenylpropyl tert.butyl	1000164-81-9	59	43.47
Silane, trichlorodocosyl-	007325-84-0	58	22.07
Pulegone	000089-82-7	53	29.65
Oxalic acid, cyclohexylmethyl propyl ester	1000309-68-1	50	27.24
7-Octenal, 3,7-dimethyl-	000141-26-4	49	30.19
Oxalic acid, cyclohexylmethyl isohexyl ester	1000309-68-3	49	28.34
Cyclopentanone, 3-methyl-2-(2-pentenyl)-	007051-39-0	49	20.39
1-Eicosanol	000629-96-9	49	22.17
6-Octen-1-ol, 3,7-dimethyl-, acetate	000150-84-5	47	30.47
Oxalic acid, cyclohexylmethyl nonyl ester	1000309-68-6	47	28.78
1,4-Benzodioxan-6-amine	022013-33-8	43	20.23
Cyclododecanol, 1-ethenyl-	006244-49-1	41	22.57
Ether, 2-phenylpropyl tert.butyl	1000164-81-9	35	59.93

## 4.2 FTIR Spectrum of the Petroleum Diesel Sample

The spectrum of the petroleum diesel sample used in this study is shown in Figure 4.3. The –OH stretch of the carboxylic acid was detected by the peak between the wavenumber of 2400 and 3300  $\text{cm}^{-1}$ .<sup>47</sup> However, this peak was not clearly observed in Figure 4.3 since it was overlapped by the peaks from the aliphatic hydrocarbon compounds between wavenumber of 2800 and 3000  $\text{cm}^{-1}$ . Also, the concentration of the carboxylic groups in petroleum diesel is much smaller than the aliphatic hydrocarbon compounds. The bending of the O-C=O group in carboxylic acid can be detected by the strong peak around 700  $\text{cm}^{-1}$ .<sup>47</sup> The deformation of the C-OH group in carboxylic acid can be detected by the peaks at around 920 and 940  $\text{cm}^{-1}$ . The peak at 1750  $\text{cm}^{-1}$  corresponds to the ester group and carboxylic acid group in the petroleum diesel sample.<sup>47</sup> The peak at the wavelength number of  $\sim 1600 \text{ cm}^{-1}$  shows that petroleum diesel contained benzene ring in the aromatic compound. The strong peak at 1460  $\text{cm}^{-1}$  concluded that there were  $\text{CH}_2$  and  $\text{CH}_3$  in the aliphatic compounds. The deprotonation of the carboxylic acid functional group in naphthenic acid depends on pH of the aqueous solution.

The presence of sulfate and O=S=O of sulfones, which are common functional groups of sulfonic acids, in the petroleum diesel can be detected by the peaks at around 1170 and 1200  $\text{cm}^{-1}$ .<sup>47</sup> The symmetric stretch of the  $\text{SO}_3$  group in the sulfonic acid can be detected by the small peak at 1060  $\text{cm}^{-1}$  position. The presence of the sulfate group in the petroleum diesel was confirmed by the GC-MS experimental results since the sulphurous acid, ester compounds contained the sulfate group. Generally, the sulfate group is surface-active. The natural surfactants containing the sulfonic acid functional groups are ionized easily and generally are independent of pH.

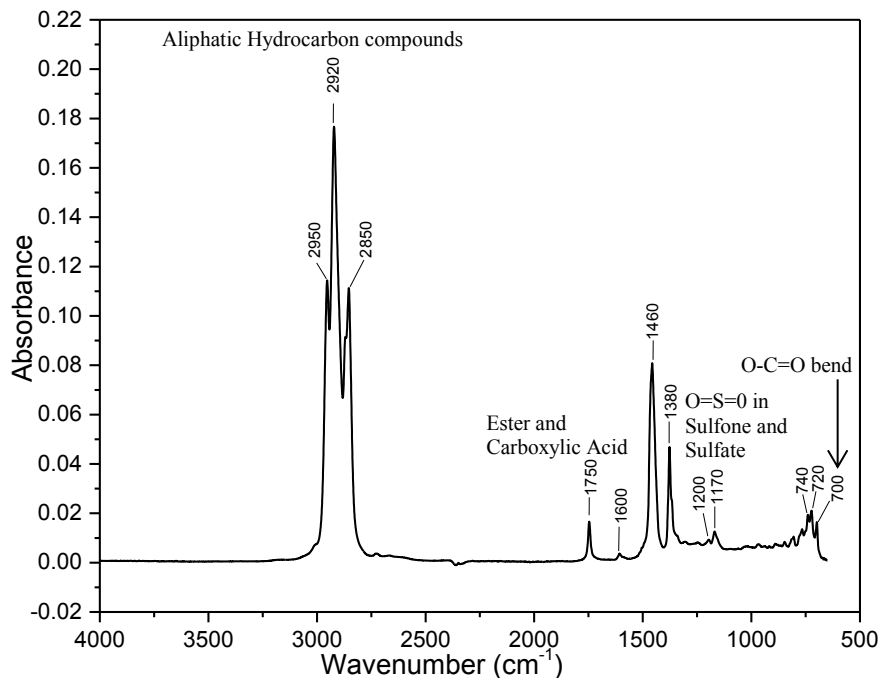


Figure 4.3: FTIR spectrum of the petroleum diesel sample.

The commercial 1-Dodecanesulfonic acid sodium salt and sodium naphthenate, which are salts of sulfonic acid and naphthenic acid (carboxylic acid), respectively, were characterized by FTIR to see whether petroleum diesel contains the sulfonic acid and carboxyl functional groups. The spectral for these commercial salts and petroleum diesel are shown in Figure 4.4. The peaks at the wavenumbers of 1050 and 1163  $\text{cm}^{-1}$  indicate the presence of sulfonic acid group in the commercial salt. The peaks at the wavenumber of 1410 and 1560  $\text{cm}^{-1}$  indicate the presence of  $\text{COO}^-$  in the carboxylic acid salts (sodium naphthenate). The strong peak at the wavenumber of 1750  $\text{cm}^{-1}$  corresponds to the presence of ester group in petroleum diesel. The peaks were detected at wavenumbers of around 1050 and 1163  $\text{cm}^{-1}$  for both petroleum diesel and 1-dodecanesulfonic acid sodium salt. The peak was detected at wavenumbers of 700  $\text{cm}^{-1}$  for both petroleum diesel and sodium naphthenate. The weak peaks could indicate a low level presence of both naphthenic acid and sulfonic acid natural surfactants in the petroleum diesel sample.

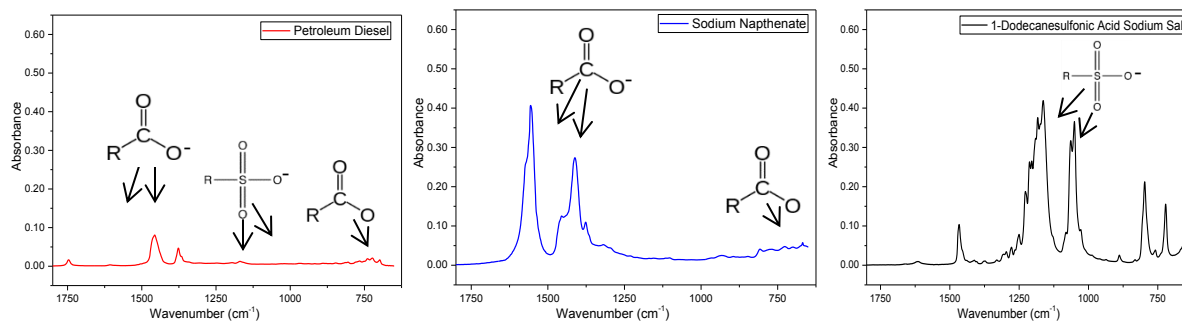


Figure 4.4: FTIR spectrum of petroleum diesel and commercial surfactant salts.

### 4.3 Surface and Interfacial Tension of Petroleum Diesel and Deionized Water

Table 4.2 shows the surface tension of deionized water and petroleum diesel as well as the corresponding interfacial tension once the interface stabilized. It can be seen from Table 4.2 that the average surface tension of deionized water was 71.82 mN/m, which is close to the literature value of 72.74 mN/m at room temperature ( $\sim 1.28\%$  experimental error).<sup>48</sup> This finding showed that the Kruss K12 tensiometer [with the Du Nouy ring method] was working properly for surface and interfacial tension measurements. The surface tension of the commercial petroleum diesel fuel was 27.82 mN/m. The experimental value of the surface tension measurement was close to the literature value of 28.0 mN/m with an experimental error of 0.64%.<sup>49</sup> The standard deviation of all repeated experimental runs for petroleum diesel was close to zero, which concludes that petroleum diesel is stable under ambient conditions.

Table 4.2: Surface tension and interfacial tension.

$\gamma_{\text{water}}$ (mN/m)	$\gamma_{\text{petroleumdiesel}}$ (mN/m)	$\gamma_{\text{water-petroleumdiesel}}$ (mN/m)
71.73	27.82	19.01
71.85	27.82	18.75
71.85	27.82	18.58
71.84	27.82	17.92
$71.82 \pm 0.06$	$27.82 \pm 0.00$	$18.57 \pm 0.46$

Another experiment was conducted to monitor the change in interfacial tension between deionized water and petroleum diesel over time. Figure 4.5 shows the dynamic change in interfacial tension between deionized water and petroleum diesel over  $\sim 3.5$  hours of measurement. The first measurement took place at 30 minutes after the initial fill of petroleum diesel to the top layer of deionized water. Interestingly, the interfacial tension between water and petroleum diesel decreased over time. A possible reason for the reduction in interfacial tension is the presence of natural surfactants in the commercial petroleum diesel, which are adsorbed at the interface. The natural surfactants of petroleum diesel were thermodynamically favoured to migrate to the interface from the bulk phase even though the migration was slow. The possible explanation for this is due to a complex mixture of hydrocarbon compounds in petroleum diesel, which can delay the migration of natural surfactants to the interface.

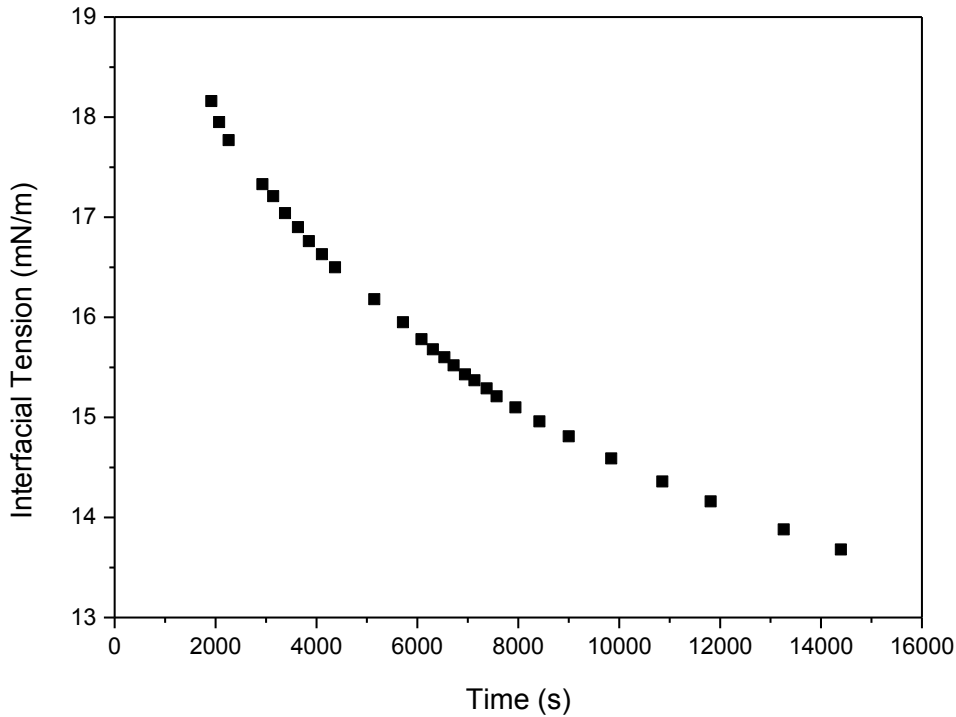


Figure 4.5: Dynamic interfacial tension between petroleum diesel and deionized water.

#### 4.4 Interfacial Tension between Petroleum Diesel and Deionized Water at Different pH

Figure 4.6 shows the interfacial tension between petroleum diesel and deionized water as a function of pH after 10 mins of initial fill. Interestingly, the interfacial tension between petroleum diesel and water stayed constant between pH of 7 and 9.5. However, the interfacial tension decreased significantly as the pH increased beyond 9.5. The measured interfacial tension was very low and the interface was hardly formed at pH 12.5 (not shown in Figure 4.6). This can be explained by the fact that there are surface active species in petroleum diesel, which are deprotonated and become more hydrophilic at high pH. As a result, these natural surfactants are thermodynamically favoured to be at the interface, which led to the lower interfacial tensions at

higher pH. The increase in pH results in ionization of the carboxylic group (R-COOH) of naphthenic acids in petroleum diesel to carboxylate (R-COO<sup>-</sup>); the ionized naphthenic acids become more hydrophilic and increase solubility in the aqueous phase.<sup>16</sup> Also, there is an accumulation of natural surfactants from the petroleum diesel bulk phase to the interface as pH increases due to increased number of carboxylic groups that are deprotonated and favourably to be migrated into the aqueous phase. The typical acid number of naphthenic acids in raw petroleum diesel is 170 mg KOH/g.<sup>50</sup>

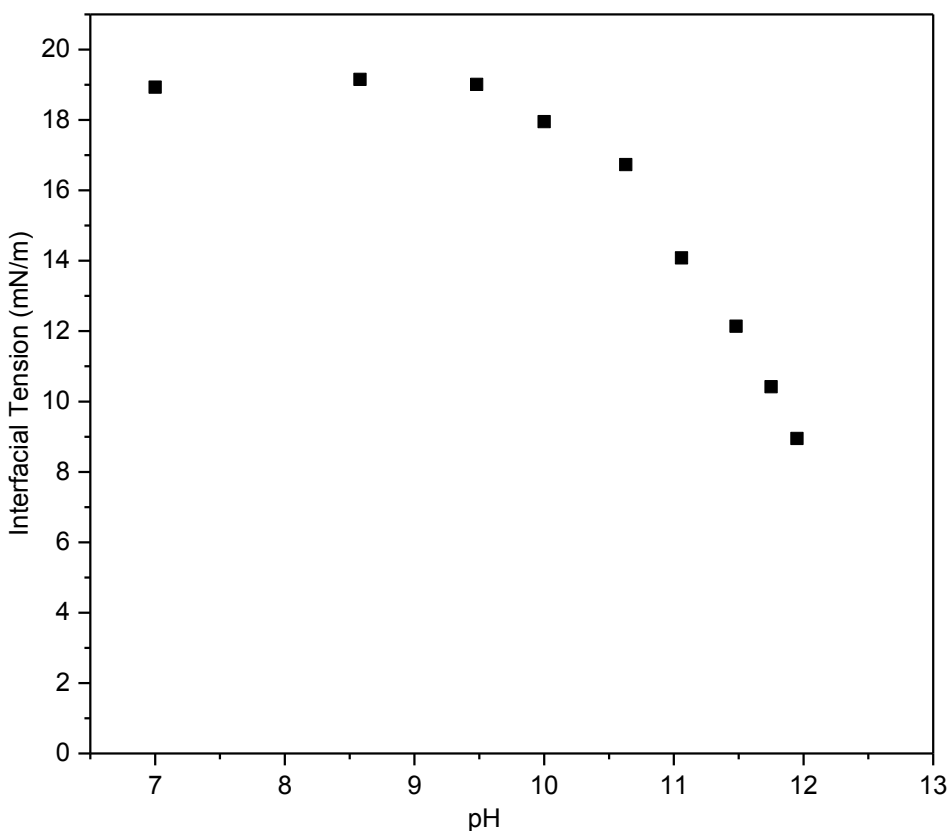


Figure 4.6: Interfacial tension between petroleum diesel and water as a function of pH.

## 4.5 Zeta Potential of Emulsified Petroleum Diesel in Electrolyte Solutions

Figure 4.7 shows the average zeta potential values of emulsified petroleum diesel in 10 mM KCl solutions at different pH. Interestingly, the isoelectric point (IEP) of emulsified petroleum diesel was around pH 2.5 compared to that at pH 3.0 for bitumen.<sup>51</sup> The IEP for all hydrocarbon compounds was found to be at pH 2.0.<sup>52</sup> Also, the IEP of dodecane, tetradecane, hexadecane, and octadecane were pH around 2.0.<sup>52</sup> Petroleum diesel contains these compounds based on GC-MS experimental results as discussed previously. It is therefore reasonable that the IEP of petroleum diesel individual hydrocarbon compounds is at pH 2.5 which is between 2.0 and 3.0.

As shown in Figure 4.7, there is a big change in the measured zeta potential of emulsified petroleum diesel between pH of 2.0 and 4.0. The trend in Figure 4.7 was similar to the trend reported for bitumen in 1 mM KCl solution in previous research work.<sup>51,53</sup> This finding indicates that petroleum diesels have similar natural surfactants as present in bitumen and might contain a combination of sulfonic, carboxylic, and protonated nitrogenous surfactants.<sup>51,54,55</sup> Also, all natural surfactants in petroleum diesel were approximately ionized and negatively charged at pH between 7 and 10. The significant change in interfacial tension between petroleum diesel and deionized water at high alkaline condition also confirms the presence of natural surfactants in petroleum diesel.

Petroleum diesel is a by-product from upgraded bitumen. Based on previous research work conducted using hexane as a model oil in the presence of sodium dodecyl sulfate, sodium palmitic acid, and dodecylamine hydrochloride surfactants in potassium chloride solution, it is possible that ionization of sulfonic, carboxylic, and nitrogenous surfactants play a major role in increasing the magnitude of zeta potential of the emulsified petroleum diesel as pH of the electrolyte solution increased in Figure 4.7.<sup>54</sup> The zeta potential obtained from the previous



research work for the fresh emulsified petroleum diesel in water after the homogenization process was  $-94.6\text{mV}$ .<sup>42</sup> The high magnitude of the measured zeta potential indicated that petroleum diesel droplets in water were stable and that the charge density of the petroleum diesel droplets was high. This indicates that petroleum diesel have natural surfactants that promote stabilization of emulsions in the aqueous environment.

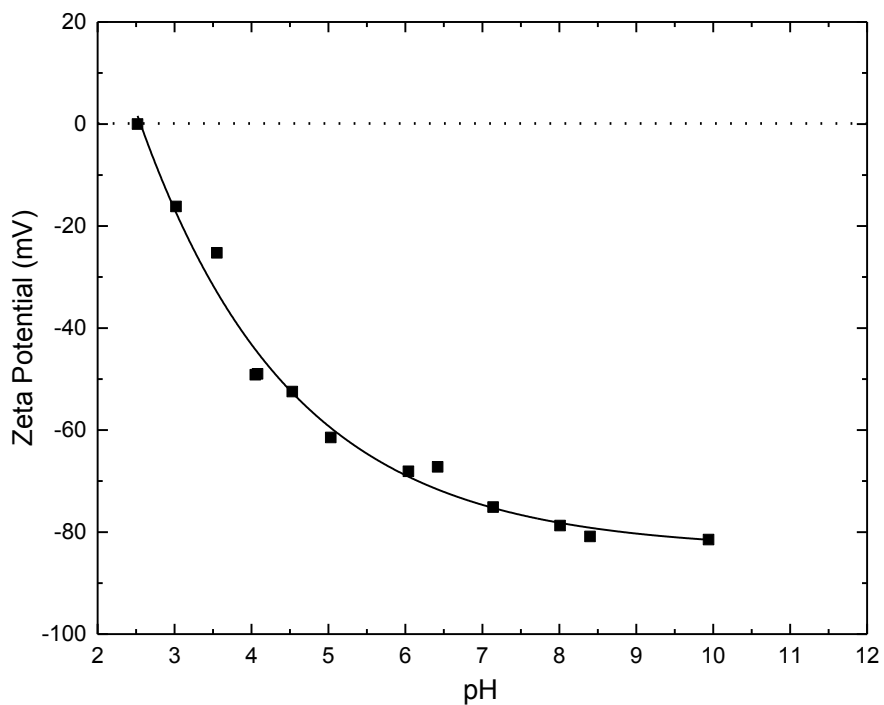


Figure 4.7: Zeta potential of emulsified petroleum diesel as a function of pH in 10 mM KCl solution.

## **Chapter 5: Results and Discussion – Industrial Research**

The batch extractor was used to evaluate the performance of petroleum diesel soaking on bitumen extraction from three different ores. A AR-G2 rheometer (TA Instruments, USA) was used to investigate the effect of petroleum diesel dosage on the viscosity of vacuum distillation feed bitumen, at temperature of  $25.00 \pm 0.05$  °C (experiment conducted by Yeling Zhu). Key experiments were conducted to investigate the effect of petroleum diesel dosages on extraction of bitumen from ores including the liberation and aeration sub-processes.

### **5.1 Bitumen Viscosity**

Figure 5.1 shows the effect of petroleum diesel dosages on the viscosity of Athabasca bitumen at an ambient condition of 25 °C. It was seen from Figure 5.1 that the viscosity decreased exponentially as the petroleum diesel dosage increased, as expected. The corresponding viscosity of diluted bitumen at petroleum diesel dosage of ~20 wt.% was 6.62 Pa·s. The experimental results in Figure 5.1 conclude that it is possible to achieve an optimal recovery of bitumen during the extraction at ambient condition of 25 °C when the bitumen viscosity is reduced to a threshold value proposed by Schram et. al. upon addition of petroleum diesel to bitumen.<sup>25</sup> The viscosity of bitumen has been shown to be one of the key parameters for achieving the optimal recovery of bitumen during the bitumen extraction of oil sands ores.<sup>20,35</sup>

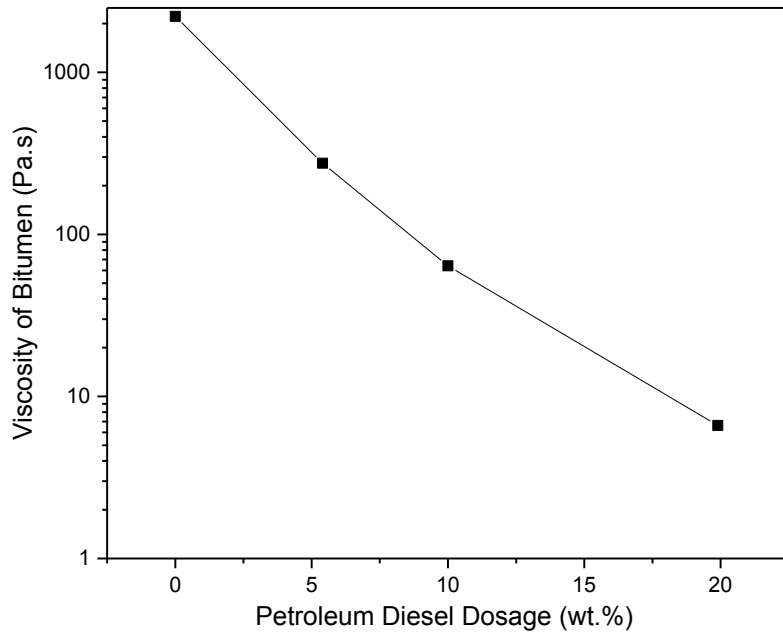


Figure 5.1: Effect of petroleum diesel dosage on bitumen viscosity (courtesy of Yeling Zhu).

## 5.2 Batch Bitumen Extraction Process

To evaluate the performance of petroleum diesel, bitumen extraction tests were conducted using a laboratory-scale Denver batch extraction unit at a constant temperature of  $25 \pm 0.5$  °C and pH of  $7.52 \pm 0.05$ . The pH of the Aurora process water was increased slightly over the flotation process. As shown in Figure 5.2 for the higher quality ore (AC ore), the quality of froth changed significantly as petroleum diesel dosages were increased during the pretreatment. The hydrocarbon content (bitumen and petroleum diesel) of the froth increased similarly, as expected. This finding indicates that the bitumen extraction performance improves when more petroleum diesel is added to the ores prior to conditioning stage of the extraction process at an ambient condition of 25 °C and the natural pH of process water without caustic soda addition (pH of  $\sim 7.52$ ). In the case of a 20 wt.% petroleum diesel dosage, the froth was oily due to high content of diluted bitumen. It was observed that there was a big difference in quality of froth produced

during the flotation from each of the three different ores at the same petroleum diesel dosage of 20 wt.%. This finding concludes that ore characteristics have an impact on froth quality. The froth quality was similar for both the high grade AD ore and the AC ore. The main reason for improvement in froth quality upon addition of petroleum diesel to the ores is likely due to a reduction in viscosity of the bitumen, which makes it easier for the diluted bitumen to float to the top of the flotation cell during the extraction process.

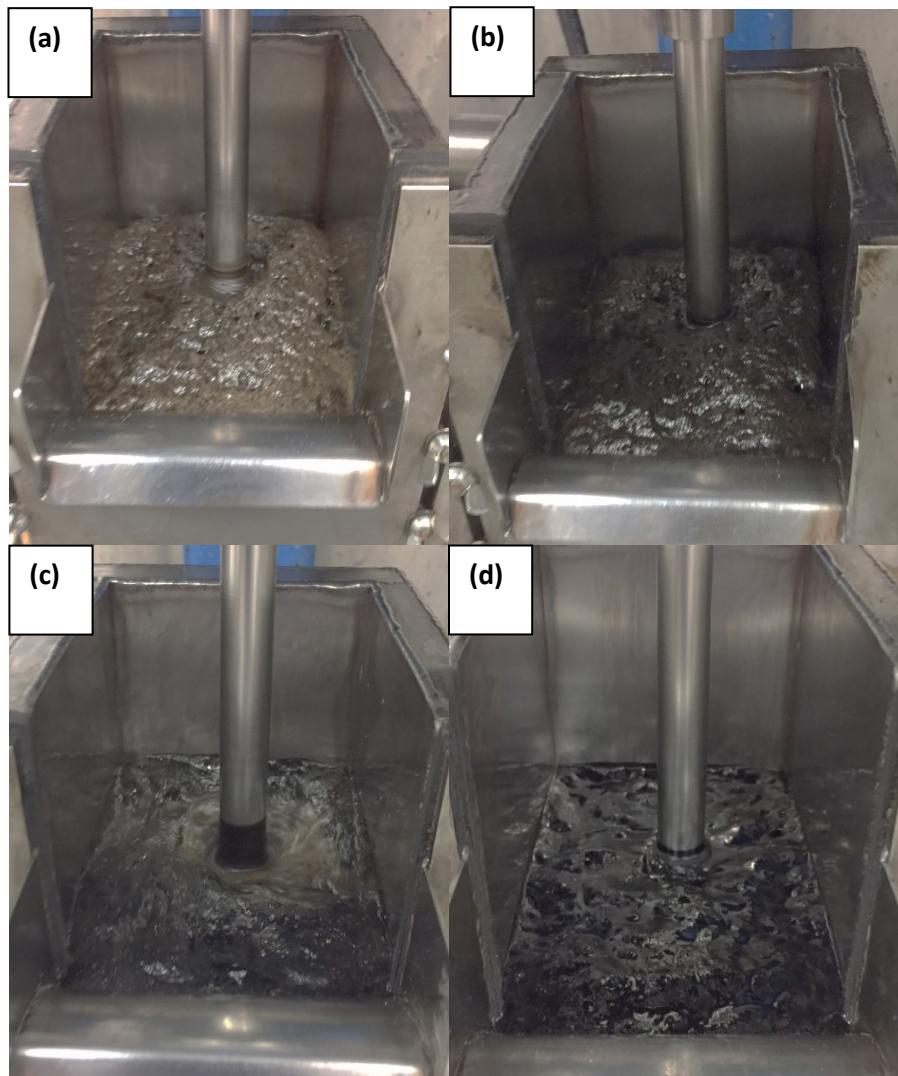


Figure 5.2: Photographs of froth from AC ore in process water slurry (a) 0 wt.% (b) 5 wt.% diesel (c) 10 wt.% diesel (d) 20 wt.% diesel.

It is interesting to note that there were about same amount of hydrocarbon compounds (bitumen and petroleum diesel) recovered from both primary and secondary froth during the flotation process for the 0 and 5 wt.% petroleum diesel addition to all of the ores. In contrast, there was much more hydrocarbon compounds in the primary froth than secondary froth for all ores at petroleum diesel dosages of 10 and 20 wt.%. This would indicate that the viscosity of bitumen was sufficiently low at these dosages to make the primary flotation process more effective. The diluted bitumen was able to flow easily during the froth collection process at the 20 wt.% petroleum diesel addition.

Dean Stark extractions were conducted to analyze the composition of froth including bitumen, petroleum diesel, water, and mineral solids. An interesting observation during the Dean Stark extractions was that there were a lot of bubbles generated in the hydrocarbon solution from the thimble containing the primary froth from the extraction experiment using the high grade AC ores and a petroleum diesel dosage of 20 wt.%.

Figure 5.3 shows the overall hydrocarbon (bitumen and diesel) recovery from both primary and secondary froth produced during the extraction processes. There was a large change in overall hydrocarbon recovery when petroleum diesel dosage was increased to 5 wt.% from 0 wt.%, which indicates that petroleum diesel is very effective for improving liberation of bitumen from ores and decreasing induction time for bitumen and air bubble attachment during the extraction process. The hydrocarbon recovery was higher for AC ore than for both AD and AK ores regardless of petroleum diesel dosage due to the higher initial bitumen content of the AC ore. It could be that the AC ore has a higher amount of bitumen natural surfactants that improves the bitumen liberation process during the extraction process. There was only marginal improvements in hydrocarbon recovery at petroleum diesel dosages of 20 wt.% as compared with that at 10

wt.% for both AD and AC ores. It is interesting to note that the hydrocarbon recovery continued to increase as the petroleum diesel dosages were increased for AK ore. The overall hydrocarbon recovery was lower at all petroleum diesel dosages in AK ores than in both AD and AC ores due to a higher amount of fines and clay in AK ore. The results in Figure 5.3 demonstrate that petroleum diesel performs well for extraction of bitumen from ores at ambient condition ( $T = 25$  °C) and a 10 wt.% petroleum diesel dosage can be used instead of 20 wt.% to achieve an optimal recovery of bitumen.

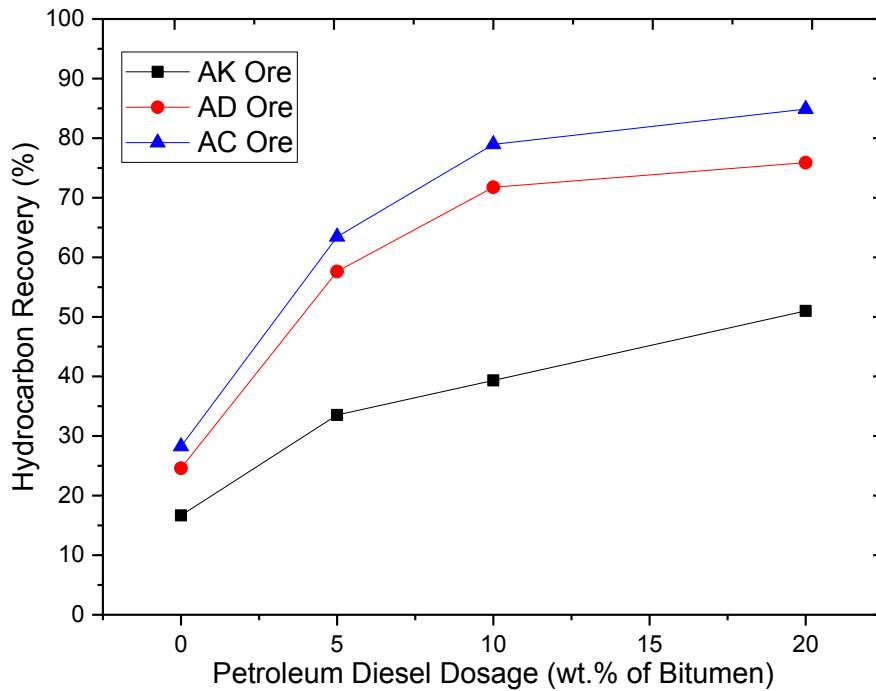


Figure 5.3: Extraction results to evaluate the performance of petroleum diesel for bitumen extraction.

Figure 5.4 shows the distribution of hydrocarbon (bitumen and diesel), water, and mineral solids in the froth after the Dean Stark extraction process. It was clear that the froth quality was poor at

all petroleum diesel dosages for the AK ore since both bitumen to mineral solids and bitumen to water weight ratios were low.

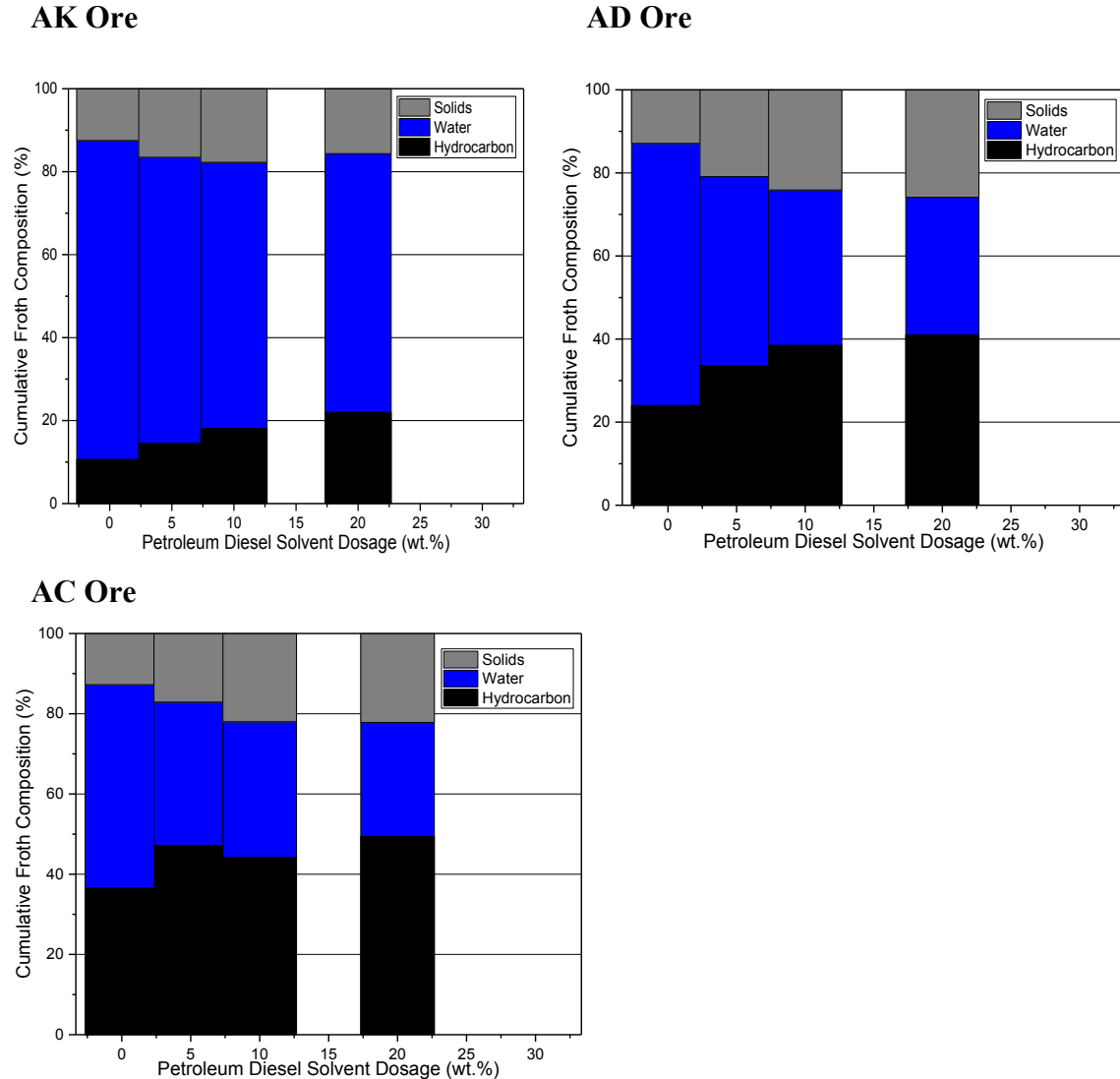


Figure 5.4: Distribution of hydrocarbon (bitumen and petroleum diesel), water, and solids in froth.

The hydrocarbon content of the froth increased as petroleum diesel dosage increased for all ores. The water content of the froth decreased with increased petroleum diesel dosage for both AD and AC ores whereas there was less change in water content of the froth for AK ore. It was

interesting to note that the mineral solids content of the froth from both AD and AC ores was generally higher than the solids content of the froth from AK ores for all diesel dosages. The increased solids contents in the froth from both AD and AC ores may indicate the entrainment of fines particles to the froth layer during the extraction process. It is seen from Figure 5.4 that the ore characteristics (grade and fines contents) and petroleum diesel dosage collectively affect the composition of froth and froth quality.

### **5.3 Comparison between Petroleum Diesel and Dodecane**

The main purpose of using dodecane in this study was to treat it as a model solvent to petroleum diesel since it contains a single hydrocarbon compound whereas petroleum diesel contains various complex hydrocarbon compounds. Extraction experiments were conducted to compare the performance between petroleum diesel and dodecane for the bitumen extraction from the AC ore.

Figure 5.5 shows the effect of solvent dosage on overall hydrocarbon recovery during the bitumen extraction process of AC ores using Aurora process water at ambient conditions (temperature of  $25 \pm 0.5^\circ\text{C}$ ) and a pH of  $7.52 \pm 0.05$ . There was very little difference in overall hydrocarbon recovery at 10 wt.% and 20 wt.% solvent dosages of petroleum diesel and dodecane. The composition of froth was also similar for both solvents as shown in Figure 5.6. The composition of hydrocarbon improved when more solvent was added to ores before the extraction in both cases. Also, the quality of froth was similar for both cases. Both petroleum diesel and dodecane have approximately the same performance on bitumen extraction process of AC ore. The similar extraction performance for both solvents indicates that the long aliphatic hydrocarbon compounds of petroleum diesel play a strong role in extraction of bitumen from ores and that both petroleum diesel and dodecane have similar solvation properties. It appears



that the low levels of natural surfactants in petroleum diesel do not play a strong role in improving the extraction process of bitumen from ores.

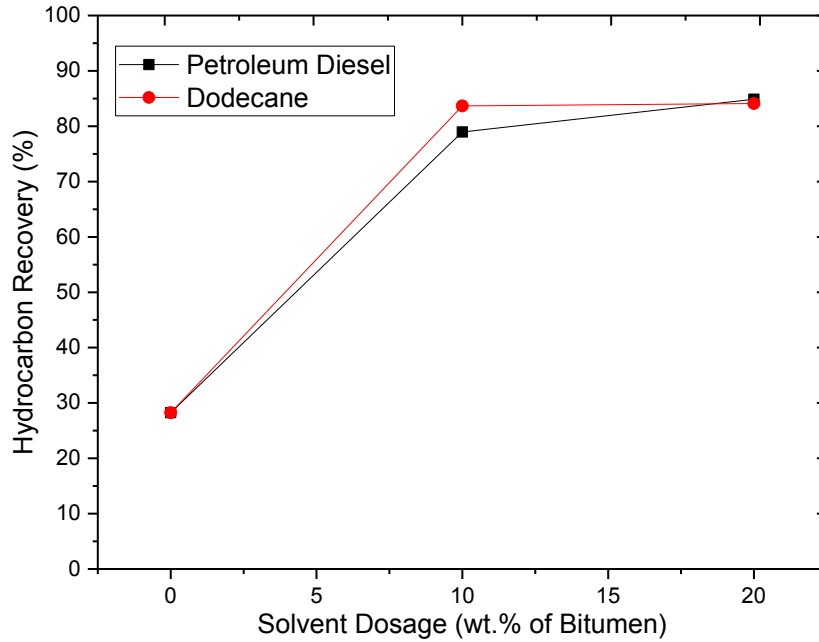


Figure 5.5: Extraction results for AC Ores using standard Denver Cell experimental protocol.

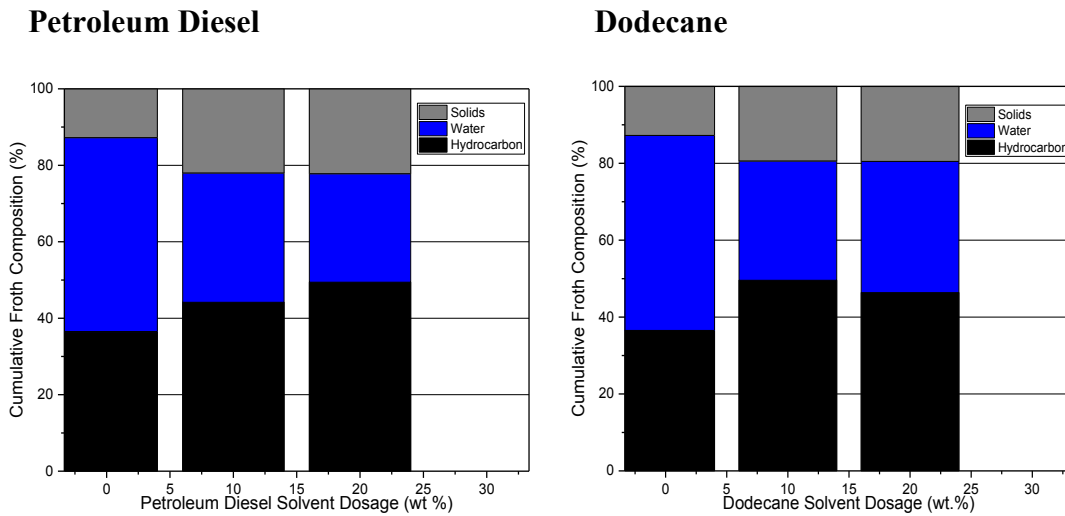


Figure 5.6: Comparison of solvent effect on froth composition of AC Ores during extraction process.

## 5.4 Bitumen Liberation Process

Figure 5.7 shows the key liberation dynamics for all three ores used in this thesis project, including the first order kinetic model fitting line with  $R^2$  values greater than 0.94. The liberation process of ores increased as dosage of petroleum diesel increased even though there was not much difference in bitumen liberation performance for all nonzero petroleum diesel dosages in the AK ore. The main reason for this is likely due to high fines content of AK ores, which trapped bitumen and made detachment of bitumen from the mineral solids more difficult. The reduction in bitumen viscosity upon addition of petroleum diesel improved the migration of bitumen natural surfactants from bulk phase to interface, resulting in lower interfacial tension between bitumen and process water. The reduction in bitumen viscosity upon addition of petroleum diesel also improves this step in the extraction process.

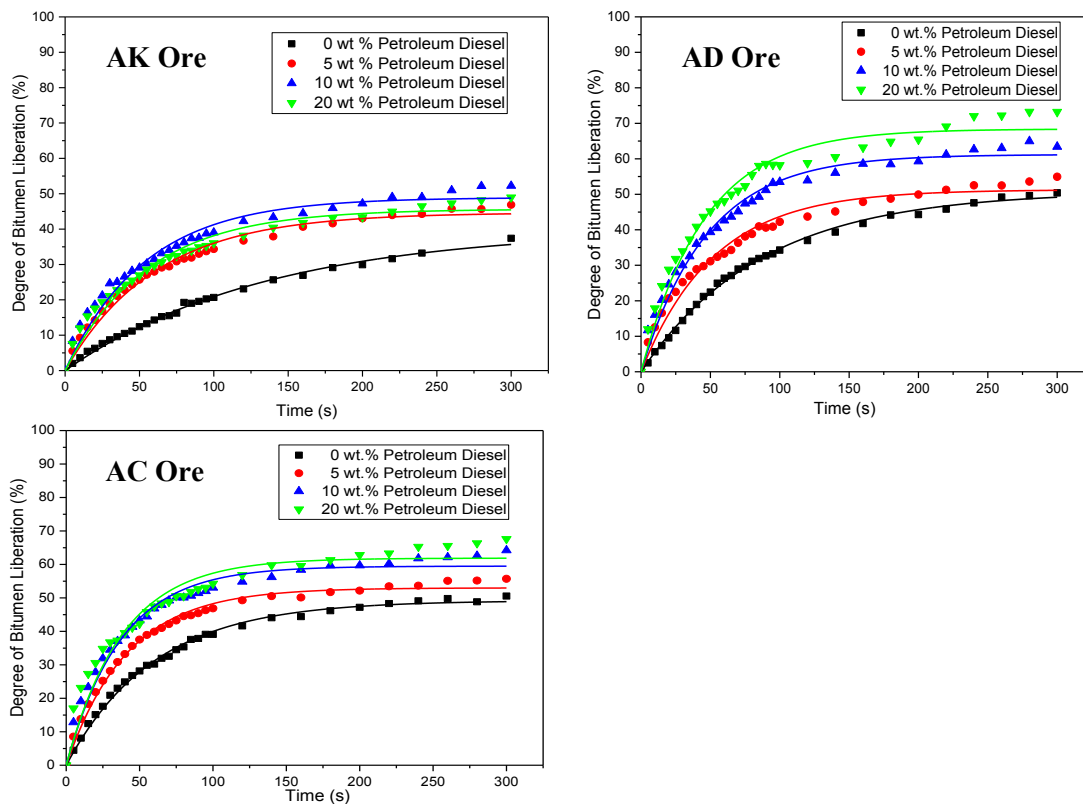


Figure 5.7: Liberation profiles of ores in Aurora process water at  $T = 25\text{ }^{\circ}\text{C}$  and pH of 7.52.

Figure 5.8 shows the calculated rate constant,  $k$ , for all ores at all solvent dosages. It is seen in Figure 5.8 that the rate constant was different for all ores at the same solvent dosage. This finding may indicate that bitumen grade and fines content of ores were the main factors that affect the rate constant of bitumen liberation. There could be higher levels of natural surfactants in the bitumen for the AD and AC ores, which might have led to the faster kinetics of the bitumen liberation process for the ores than AK ore. It was seen in Figure 5.8 that the solvent improves the bitumen liberation performance for all ores since the liberation rate constant was generally higher. There was only a marginal improvement in liberation performance from 10 wt.% solvent addition to 20 wt.% solvent addition, which was consistent with the results of bitumen extraction mentioned earlier. This finding indicates that a 10 wt.% solvent dosage may approximate an optimum dosage. Overall, the solvent dosage, ore grade, and fines content of ores are the main factors that affect the bitumen liberation performance of ores during the extraction process.

Figure 5.8 also provides comparison between the petroleum diesel and dodecane solvents. It is seen in Figure 5.8 that the rate constant of the bitumen liberation process was about the same for both solvent cases. This indicates that there were sufficient natural surfactants in bitumen that play a strong role in controlling the liberation process regardless the type of solvent used. The results in Figure 5.8 suggest that it may not be necessary to buy external chemical additives at ambient condition of 25°C and natural pH of ~7.52 in process water. The similar results for these two solvents confirm that the natural surfactants in petroleum diesel did not play a strong role in liberation of bitumen from ores and that the reduction in bitumen viscosity is the main reason for improvement in bitumen liberation from ores upon the addition of the solvent.

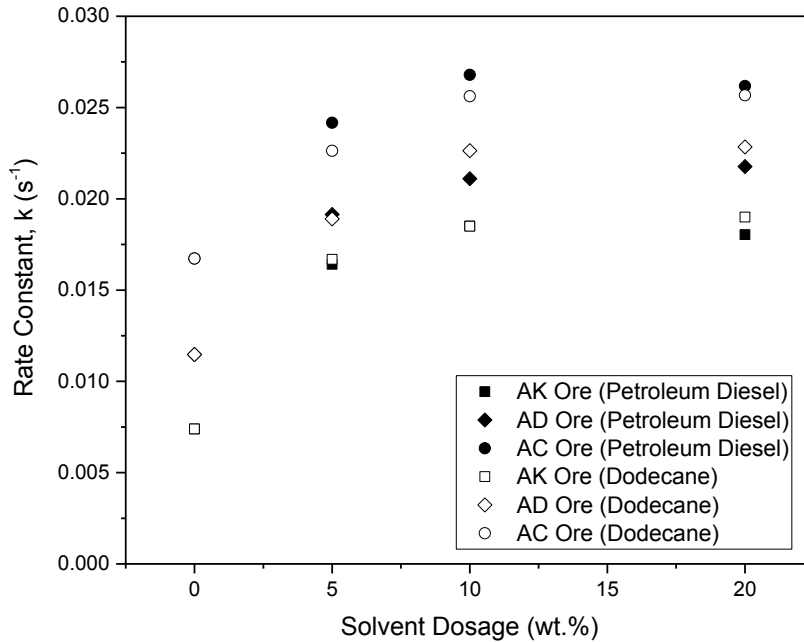


Figure 5.8: Effect of solvent dosage on liberation performance of various ores.

## 5.4 Bitumen Aeration Process

Figure 5.9 shows the attachment probability profiles at all petroleum diesel dosages in process water at ambient conditions of  $25 \pm 1$  °C and constant pH of  $7.52 \pm 0.05$ . The fitting of polynomial curve was used to obtain the induction time (50% attachment). There was not much difference in induction time (50% attachment) for 10 wt.% and 20 wt.% petroleum diesel addition. This finding was consistent with the extraction and bitumen liberation results at the same operating conditions. Figure 5.10 shows the effect of petroleum diesel addition on induction time for bitumen and air bubble attachment. Again, there was marginal reduction in induction time upon addition of 20 wt.% petroleum diesel as compared with 10 wt.% petroleum diesel addition. All the results in Figures 5.9 and 5.10 conclude that petroleum diesel is effective for improving aeration process of bitumen, leading to a decrease in induction time for bitumen and air bubbles attachment. The main contribution to the improved aeration process is likely due

to the reduction in bitumen viscosity, which makes spreading of bitumen around air bubbles easier. Similar induction time results were obtained for the case of kerosene (temperature of 35 °C and pH of 8.5) in previous research work conducted.<sup>19</sup>

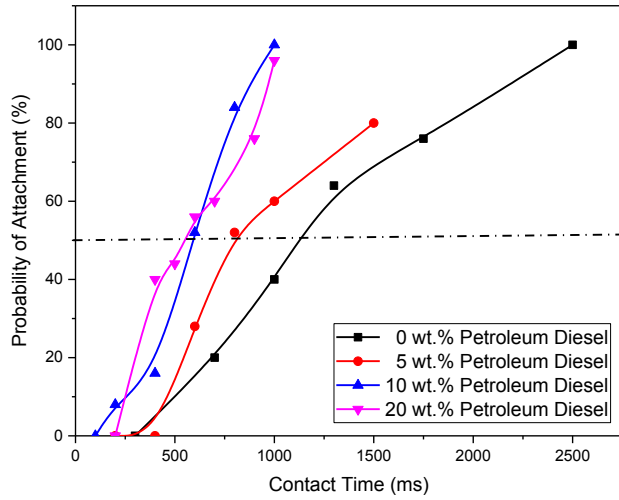


Figure 5.9: Probability profile of air bubble-bitumen attachment over the contact time between bitumen and air bubble.

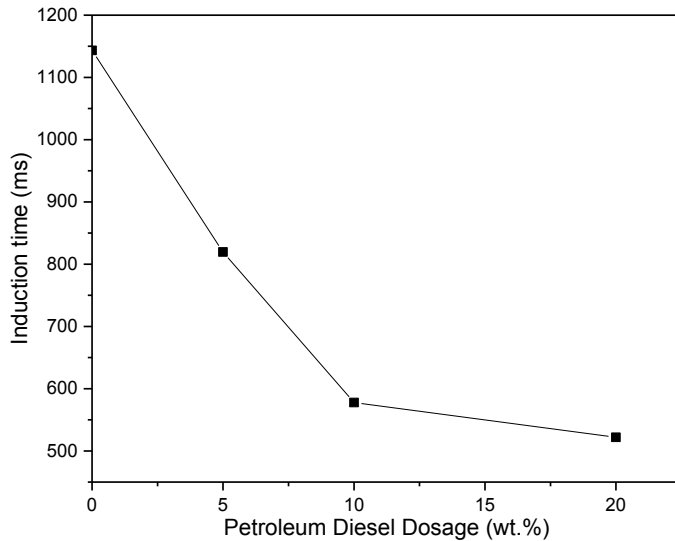


Figure 5.10: Induction time as a function of petroleum diesel dosage.

Figure 5.11 shows the probability profile for attachment between air bubbles and bitumen with/without fines particles. The calculated induction time based on the polynomial fitting curve was 6635 m.s for the fine-coated bitumen in Aurora process water. The calculated induction time is very similar to the results obtained in previous research work using similar experimental conditions (25 °C and 0.5 wt.% fines in presence of 50 ppm  $\text{Ca}^{2+}$ ).<sup>26</sup> The calculated induction time in Figure 5.11 was five times higher for fines-coated bitumen than that for bitumen without fines particles (~1140 m.s). The presence of divalent cations ( $\text{Ca}^{2+}$  and  $\text{Mg}^{2+}$ ) in the process water can result in slime coating of bitumen by fine particles. Calcium and magnesium ions act like a binder between the carboxylic acid of bitumen and fine particles.<sup>26</sup> As a result, the bitumen becomes more hydrophilic, which makes attachment between bitumen and air bubbles more difficult. This implies that the overall hydrocarbon recovery during the bitumen extraction process using AK ores (43 wt.% fines) was lower as anticipated due to increased induction time during the aeration process than the case of AD and AC ores.<sup>26</sup>

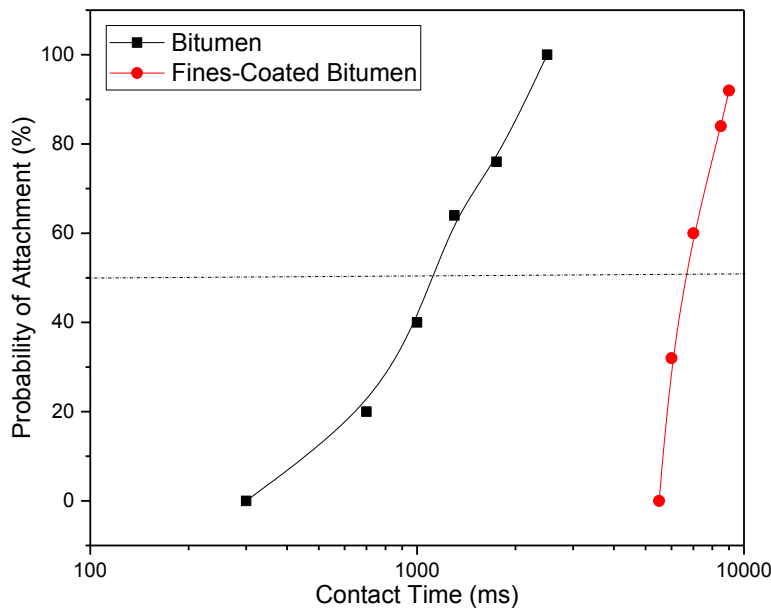


Figure 5.11: Comparison of aeration process between bitumen and fines-coated bitumen.

## Chapter 6: Solvent Loss to Tailings

### 6.1 Objective

The main goal of this section is to analyze the loss of petroleum diesel to tailings produced from the bitumen extraction process. The other goal is to check whether the loss of petroleum diesel to tailings meet the regulatory specification for loss of solvent to tailings. The study is limited to analysis of solvent in froth and residual in tailing solids.

### 6.2 Preliminary Experiment (Petroleum Diesel)

The preliminary experiment was conducted using a TGA Q500 (TA Instruments, Canada) instrument and soaked solid samples (~2 wt.% petroleum diesel and ~8 wt.% bitumen). As shown in Figure 6.1, there is no clear peak in the differential curve for petroleum diesel. This suggests that the weight loss of the samples is due to evaporation of petroleum diesel and bitumen lighter compounds at the same time at lower temperature range. It is therefore difficult to differentiate petroleum diesel from bitumen for quantitative analysis. Also, both petroleum diesel and bitumen lighter components have similar chemical compounds.

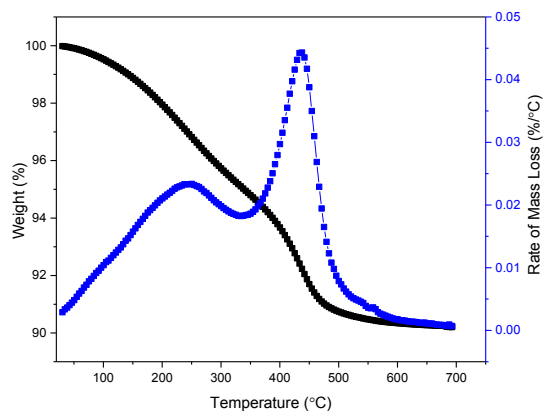


Figure 6.1: TGA profile of solids and hydrocarbon sample (~2 wt.% petroleum diesel and ~8 wt.% bitumen).

The challenge above motivates the use of dodecane as a model solvent to petroleum diesel for quantitative analysis. Petroleum diesel contains dodecane as confirmed by GC-MS experiment mentioned earlier. Also, both petroleum diesel and dodecane solvent addition to oil sands ores were shown to have approximately the same performance on bitumen extraction of AC ores mentioned earlier in Chapter 5.3. The method for dodecane loss to tailings solids generated after the bitumen extraction process of AC ores is in the following section.

### **6.3 Method of Solvent Loss Analysis**

A Dean Stark apparatus was used to extract bitumen (and dodecane) from water and solids in the froth and tailings solids using toluene as the refluxing agent after the standard extraction experiments were conducted for the AC ore (see Table 3.2) at 10 and 20 wt.% dodecane addition (with respect to bitumen content in ores). This provided a comparison between dodecane and petroleum diesel on the bitumen extraction process of ores at ambient condition. The dodecane experiments were used to predict the petroleum diesel loss to tailings. The collected hydrocarbon solution was saved for all thermogravimetric analysis (TGA) experiments.

A TGA Q500 (TA Instruments, Canada) instrument was used to analyze dodecane in froth and residuals in tailing solids. A platinum pan was used as a sample holder. The furnace was purged with the nitrogen gas throughout the balance and the sample location at 40 mL/min and 60 mL/min gas flow rates, respectively. The furnace was heated at a constant rate of 10°C/min to a temperature of 150°C for froth samples and 700°C for tailings solids samples. The nitrogen gas was used to remove dodecane and bitumen from the samples. The cleaned AC ore sample and ~10 wt.% of Dean Stark hydrocarbon solutions were used to prepare TGA samples. The weight of each sample was between 25 and 100 mg for all TGA experiments. All experiments were conducted several times at each condition. Additional TGA experiments were conducted using



cleaned AC solids and dodecane samples to determine the temperature at which dodecane was completely evaporated. Figure 6.2 shows the typical diagram of the TGA apparatus.

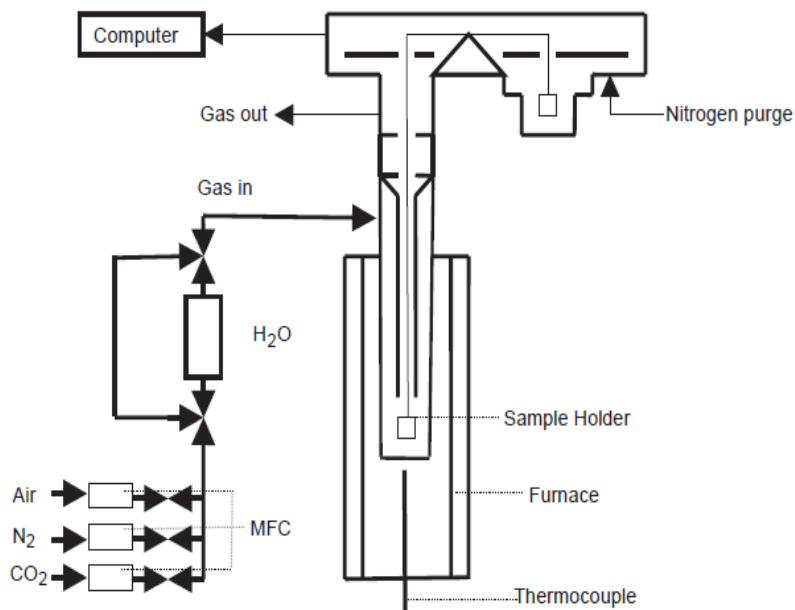


Figure 6.2: Typical schematic diagram of the TGA apparatus.<sup>56</sup>

### 6.3 Results and Discussion

Experiments were conducted using Thermogravimetric Analysis (TGA) to determine the temperature at which dodecane was completely evaporated. Toluene was also examined since it was used in the Dean Stark extractions. Samples for analysis were prepared as described in the previous section. Toluene was completely evaporated before 35 °C whereas there was negligible weight loss of dodecane at the same temperature, as shown in Figure 6.3. It was found that dodecane was completely evaporated before 110 °C. Therefore, the mass loss up to 110 °C was used to calculate the dodecane content in the bitumen for all remaining TGA experiments. Interestingly, both toluene and dodecane were evaporated completely at temperatures lower than the normal boiling point of 110 °C and 216 °C for toluene and dodecane, respectively. This is

likely due to purging of nitrogen gas that removes toluene and dodecane easily from the sample during the TGA experiment.

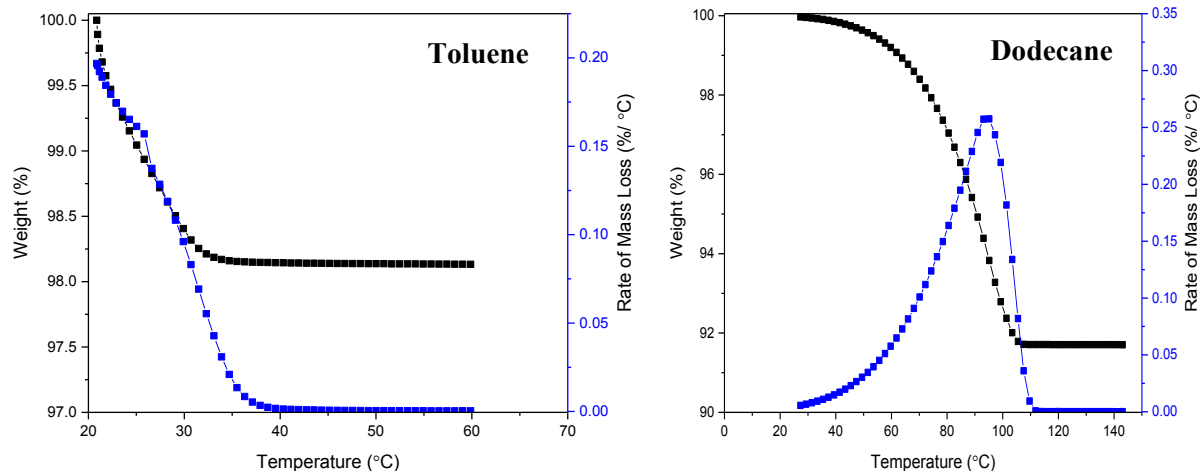


Figure 6.3: TGA profile of AC solid soaked with solvent.

Figure 6.4 shows the comparison between AC solids soaked with bitumen and 2 wt.% solvents (50/50 toluene:dodecane and dodecane only) samples. It is seen in Figure 6.4 that all dodecane has evaporated before 110 °C and the corresponding weight loss was ~1 wt.% and ~2 wt.% for toluene:dodecane and dodecane case, respectively. This finding shows that TGA can be used to separate dodecane from toluene and bitumen for analysis. Also, these experiments confirm that toluene easily evaporated from the sample prior to TGA experiments. The weight loss was mainly due to decomposition of bitumen after 110 °C. The bitumen was converted to coke and ash at higher temperatures. Again, weight loss up to  $110.0 \pm 0.2$  °C was used to analyze the dodecane content in hydrocarbon (HC) including the correction factor of small weight loss due to evaporation of saturated hydrocarbon compounds in bitumen (0.0195%) for the froth layer case.

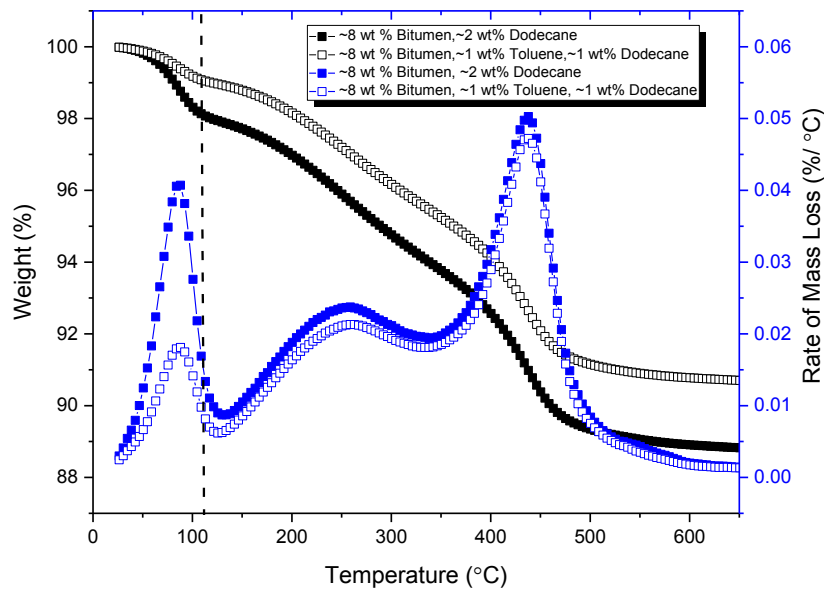


Figure 6.4: TGA profile of AC solid sample.

Figure 6.5 (a) shows the example of the TGA profile for Dean Stark hydrocarbon solution of the primary froth produced during the extraction experiment for the case of 20 wt.% dodecane addition. The peak for dodecane and traces of bitumen saturate hydrocarbon compounds was clearly observed up to 90 °C. The majority of weight loss at temperatures higher than 300 °C was due to decomposition of the heavy bitumen components such as asphaltenes in the hydrocarbon solution of the tailings solids in Figure 6.5 (b).<sup>57</sup> There was a very small change in weight of the sample before 110°C for the tailings solids case, which indicated that amount of residual dodecane in the Dean Stark hydrocarbon solution (tailings solids case) was low.

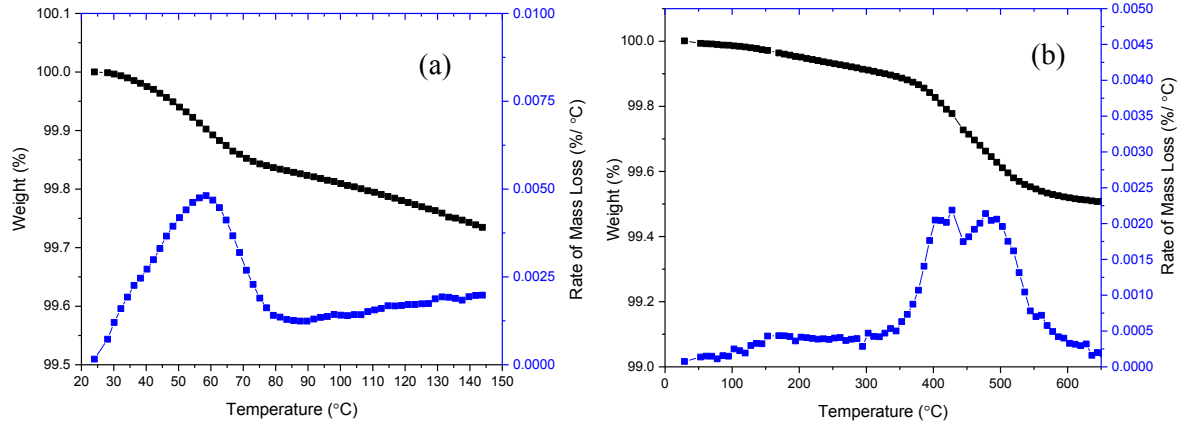


Figure 6.5: TGA profile of (a) primary froth and (b) tailings solids produced during extraction (20 wt.% dodecane case).

Table 6.1 shows the key summary for analysis of dodecane in froth layer after the extraction experiment was conducted using the AC ore at different dodecane dosages. It is seen from Table 6.1 that majority of dodecane was in the froth; therefore the solvent loss to tailings would be low. As shown in Table 6.1, the ratio of dodecane to bitumen in total froths is higher than the initial state for 10 and 20 wt.% cases. This suggests that dodecane prefers to stay with bitumen, rather than water or solids during the bitumen extraction process of ores. The ratio of dodecane to bitumen in the secondary froth for the case of 20 wt.% dodecane dosage is slightly higher than that in the primary froth. This finding suggests that 20 wt.% dodecane is overdose. To minimize solvent loss, it would be best to use 10 wt.% solvent dosage since there is diminishing improvement in bitumen recovery when 20 wt.% solvent dosage is used instead of 10 wt.% for bitumen extraction at ambient condition (temperature of 25 °C).

Table 6.1: Summary of dodecane in froth determined by TGA.

Dodecane Dosage (wt.%)	10			20		
	Bitumen (g)	Dodecane (g)	Dodecane / Bitumen Ratio	Bitumen (g)	Dodecane (g)	Dodecane / Bitumen Ratio
Initial State	57.06	5.70	~10%	57.04	11.39	~20%
Primary Froth	41.81	4.48	10.71%	37.41	7.53	20.14%
Secondary Froth	5.98	0.52	8.71%	9.97	2.34	23.53%
Total Froths	47.79	5.00	10.46%	47.37	9.88	20.85%
Final Tailings*	9.27	0.70	7.56%	9.67	1.51	15.65%
<b>Overall Recovery in Froth (wt.%)</b>	<b>83.75</b>	<b>87.70</b>	-	<b>83.05</b>	<b>86.72</b>	-

\*Estimated based on calculation from mass balance (not measured)

Table 6.2 shows the summary for the loss of dodecane to the tailings solids layer during the extraction experiments for both 10 and 20 wt.% dodecane dosage cases. The ratio of dodecane to bitumen in the tailings solids is much lower for both 10 and 20 wt.% cases than that for total froths in Table 6.1, which suggests that the solvent loss to tailings solids can be reduced by recovering more bitumen from tailings solids. The loss of solvent per 1000 barrels of bitumen produced was lower than the specification (4 barrels of solvent per 1000 barrels of bitumen produced) for both cases.<sup>8</sup> Harjai et al. suggested that recycling process water from tailing ponds would help reduce the solvent loss to tailings based on experiments conducted to determine the kerosene content in tailing waters.<sup>19</sup>

Table 6.2: Summary in loss of dodecane to tailings solids.

Dodecane Dosage (wt.%)	10	20
Initial Addition of Dodecane (g)	5.70	11.39
Dodecane in Tailings Solids (g)*	0.12	0.13
Loss of Dodecane to Tailings Solids (wt.%)	2.04	1.12
Bitumen in Bottom Tailings Solids (g)	5.02	3.68
Dodecane/Bitumen Ratio (wt.%)	2.32	3.47
Recovered Bitumen (g)	47.79	47.37
Net Bitumen Recovery (wt.%)	83.75	83.05
Loss of Solvent (Barrels per 1000 Barrels of Bitumen Produced)	2.44	2.70

\*Estimated from TGA experiments based on method developed for measuring dodecane content.

## 6.4 Conclusions

The hybrid bitumen extraction process of ores can meet the solvent loss specification when petroleum diesel or dodecane is used as solvent based on quantitative experimental results of dodecane in the tailing solids. To minimize solvent loss, it would be best to use 10 wt.% solvent dosage since there is diminishing improvement in bitumen recovery when 20 wt.% solvent dosage is used instead of 10 wt.% for bitumen extraction at ambient condition (temperature of 25 °C). A reduced concentration of dodecane in bitumen was observed with increased difficulty in bitumen recovery for the 10 wt.% dodecane dosage case; this trend suggests that solvent loss to tailings can be reduced by recovering more bitumen.

## Chapter 7: Conclusions

In this research, three oil sand ores provided by Syncrude were used to evaluate the performance of petroleum diesel for the extraction of bitumen at ambient conditions. Various analytical techniques were used to understand efficiency of petroleum diesel when used as a solvent for the bitumen extraction process at ambient conditions and to develop some insight as to how this solvent works to improve bitumen recovery.

Petroleum diesel contains a mixture of aliphatic and aromatic hydrocarbon compounds as confirmed by analysis using gas chromatography/mass spectrometry and fourier transform infrared spectroscopy. These techniques also confirmed the presence of surfactant active functional groups in petroleum diesel. Petroleum diesel was found to contain low levels of natural surfactants (mainly naphthenic acids), as confirmed by interfacial tension and zeta potential measurement results at various pH. The deprotonation of the carboxylic functional groups in naphthenic acids of petroleum diesel was observed at high pH. The presence of various hydrocarbon compounds in petroleum diesel improves the miscibility of bitumen and extraction efficiency of bitumen from oil sands ores at ambient conditions.

Based on flotation experimental results, increases in grade and decreases in fines content of the ores led to high hydrocarbon recovery during the extraction process as a function of petroleum diesel dosage. Petroleum diesel performs well for the extraction of bitumen from ores at ambient temperature (25 °C), leading to high bitumen recovery. Both petroleum diesel and dodecane were shown to have approximately the same performance on bitumen liberation process of ores and overall bitumen extraction process of high grade ores, which shown that the natural surfactants in petroleum diesel didn't play a strong role in improving the liberation process of

bitumen from ores. The experimental results suggest that interfacial tension is an important parameter for the liberation of bitumen from ores by reducing bitumen viscosity, which facilitates the migration of bitumen natural surfactants to the interface between bitumen and water in the presence of an organic solvent. The loss of petroleum diesel to tailings solids was shown to be small and met the regulatory specification for solvent loss to tailings solids based on the experimental results using dodecane as a model solvent to petroleum diesel.

The bitumen liberation kinetics improved when more petroleum diesel was added to ores prior to the liberation process of bitumen from ores. There was a diminishing improvement in the liberation process when petroleum diesel dosage was increased to 20 wt.% from 10 wt.%. The addition of petroleum diesel to bitumen led to reductions in induction time for bitumen and air bubbles attachment and therefore, to improve aeration efficiencies of bitumen. However, the presence of fines in ores led to bigger issues in the aeration process than the liberation process, likely due to the formation of bonds between bitumen natural surfactants and fine particles in the presence of divalent cations, resulting in the bitumen more hydrophilic and attachment between bitumen and air bubbles more difficult.

Overall, the novel concept of using petroleum diesel as a solvent for a hybrid aqueous-nonaqueous bitumen extraction process was validated with an optimal petroleum diesel dosage of approximately 10 wt.% based on the experimental results. Additional research work is required before this novel concept can be applied commercially at the industrial site.



## **Chapter 8: Contribution to Original Knowledge**

There were several key research outcomes from the work conducted for this thesis project:

- The effect of pH on interfacial tension between petroleum diesel and water was investigated to confirm the low level presence of surface active species. A comparison between petroleum diesel and dodecane on the bitumen liberation process of ores determined that the natural surfactants in petroleum diesel did not play a strong role in liberation process of bitumen from ores.
- Petroleum diesel was shown to be an effective solvent for extraction of bitumen from ores to evaluate the novel concept of aqueous-nonaqueous hybrid bitumen extraction process of ores.
- The effective use of TGA techniques to analyze the dodecane content in froth and tailings solids was developed. The solvent loss to the tailings solids was shown to meet the regulatory specification.

## **Chapter 9: Future Research**

In this thesis research, petroleum diesel was shown to be an effective solvent for hybrid aqueous-nonaqueous bitumen extraction process. However, there are many other factors that play a role in bitumen extraction process of ores such as the chemistry of bitumen, solvent types, and interfacial properties between various components in the system. Petroleum diesel was shown to have insufficient amount of natural surfactants for improving bitumen extraction process of ores. The various hydrocarbon composition of petroleum diesel can affect the efficiency of petroleum diesel for bitumen extraction of oil sands ores. The level of natural surfactants in the petroleum

diesel can have an impact on the bitumen extraction efficiency including the liberation and aeration sub-processes. The following suggestions for future research can be conducted before the novel concept of hybrid aqueous-nonaqueous bitumen extraction process can be applied commercially at the industrial site:

1. The use of chemical additives with petroleum diesel should be studied at 25 °C to determine whether it further improves processability and increases robustness of the bitumen extraction process. It would also be valuable to study whether controlling the pH of the process water improves the liberation and aeration sub-processes for this case.
2. The comparison between light and heavy petroleum diesel on bitumen extraction performance of ores may be investigated to determine the effect of solvent types on bitumen extraction.
3. One could study the aeration process using the induction timer device to investigate the effect of pH on induction time for air bubble and diluted bitumen (with petroleum diesel) attachment.
4. The induction time and viscosity measurements of bitumen from various ores using centrifugation methods would be valuable to determine whether the bitumen chemistry from different sources affect the efficiency for extraction of bitumen from ores.

## References

- (1) Srinivasa, S.; Flury, C.; Afacan, A.; Masliyah, J.; and Xu, Z. Study of Bitumen Liberation from Oil Sands Ores by Online Visualization. *Energy Fuels* **2012**, *26*, 2883-2890.
- (2) Takamura, K. Microscopic Structure of Athabasca Oil Sand. *Can. J. Chem. Eng.* **1982**, *60*, 538-545.
- (3) He, L.; Lin, F.; Li, X.; Sui, H.; Xu, Z. Interfacial Sciences in Unconventional Petroleum Production: From Fundamentals to Applications. *Chem. Soc. Rev.* **2015**, *44*, 5446-5494.
- (4) Flury, C.; Afacan, A.; Bakhtiari, M. T.; Sjoblom, J.; Xu, Z. Effect of Caustic Type on Bitumen Extraction from Canadian Oil Sands. *Energy Fuels* **2014**, *28*, 431-438.
- (5) Masliyah, J.; Zhou, Z.; Xu, Z.; Czarnecki, J.; Hamza, H. Understanding Water-Based Bitumen Extraction from Athabasca Oil Sands. *Can. J. Chem. Eng.* **2004**, *82*, 628-654.
- (6) Alberta Energy Regulator Crude Bitumen Demand - Upgraded & Nonupgraded Bitumen. <https://www.aer.ca/data-and-publications/statistical-reports/crude-bitumen-demand> **(accessed 05/17, 2017)**.
- (7) Long, J.; Xu, Z.; Masliyah, J. H. On the Role of Temperature in Oil Sands Processing. *Energy Fuels* **2005**, *19*, 1440-1446.
- (8) Wu, J.; Dabros, T. Process for Solvent Extraction of Bitumen from Oil Sand. *Energy Fuels* **2012**, *26*, 1002-1008.

- (9) Mohebati, M. H.; Maini, B. B.; Harding, T. G. In *Experimental Investigation of the Effect of Hexane on SAGD Performance at Different Operating Pressures*; SPE Heavy Oil Conference Canada held in Calgary, Alberta, Canada, June 12-14, 2012. Society of Petroleum Engineers: **2012**.
- (10) Bao, Y.; Wang, J.; Gates, I. D. On the Physics of Cyclic Steam Stimulation. *Energy* **2016**, *115, Part 1*, 969-985.
- (11) Zawala, J.; Dabros, T.; Hamza, H. A. Settling Properties of Aggregates in Paraffinic Froth Treatment. *Energy Fuels* **2012**, *26*, 5775-5781.
- (12) Ferguson, G. P.; Rudolph, D. L.; Barker, J. F. Hydrodynamics of a Large Oil Sand Tailings Impoundment and Related Environmental Implications. *Can. Geotech. J.* **2009**, *46*, 1446-1460.
- (13) Wang, X. T.; Feng, X.; Xu, Z.; Masliyah, J. H. Polymer Aids for Settling and Filtration of Oil Sands Tailings. *Can. J. Chem. Eng.* **2010**, *88*, 403-410.
- (14) Alamgir, A.; Harbottle, D.; Masliyah, J.; Xu, Z. Al-PAM Assisted Filtration System for Abatement of Mature Fine Tailings. *Chem. Eng. Sci.* **2012**, *80*, 91-99.
- (15) Mahmoudkhani, A.; Fenderson, T.; Watson, P.; Wu, Y.; Nair, M. In *New Environmental Friendly Process Aids Improve Bitumen Recovery and Accelerate Tailings Settling of Low-Grade Oil Sands*; SPE Hydrocarbon, Economics, and Evaluation Symposium held in Calgary, Alberta, Canada, September 24–25, 2012. Society of Petroleum Engineers: **2012**.

- (16) Masliyah, J. H.; Xu, Z.; Czarnecki, J. A.; Dabros, M. In *Handbook on Theory and Practice of Bitumen Recovery from Athabasca Oil Sands*; Kingsley Knowledge Pub: Cochrane, Alta., **2011**, Vol. 1.
- (17) Li, X.; Sun, W.; Wu, G.; He, L.; Li, H.; Sui, H. Ionic Liquid Enhanced Solvent Extraction for Bitumen Recovery from Oil Sands. *Energy Fuels* **2011**, *25*, 5224-5231.
- (18) Painter, P.; Williams, P.; Mannebach, E. Recovery of Bitumen from Oil or Tar Sands using Ionic Liquids. *Energy Fuels* **2010**, *24*, 1094-1098.
- (19) Harjai, S. K.; Flury, C.; Masliyah, J.; Drelich, J.; Xu, Z. Robust Aqueous-Nonaqueous Hybrid Process for Bitumen Extraction from Mineable Athabasca Oil Sands. *Energy Fuels* **2012**, *26*, 2920-2927.
- (20) He, L.; Lin, F.; Li, X.; Xu, Z.; Sui, H. Enhancing Bitumen Liberation by Controlling the Interfacial Tension and Viscosity Ratio through Solvent Addition. *Energy Fuels* **2014**, *28*, 7403-7410.
- (21) Neumann, H.; Paczynska-Lahme, B.; Severin, D. In *Composition and Properties of Petroleum*; Geology of Petroleum; Halsted Press and Wiley Ltd.: New York and Chichester, **1981**, Vol.5.
- (22) He, L.; Li, X.; Wu, G.; Lin, F.; Sui, H. Distribution of Saturates, Aromatics, Resins, and Asphaltenes Fractions in the Bituminous Layer of Athabasca Oil Sands. *Energy Fuels* **2013**, *27*, 4677-4683.

- (23) Wang, S. Q.; Liu, J. J.; Zhang, L. Y.; Masliyah, J.; Xu, Z. H. Interaction Forces between Asphaltene Surfaces in Organic Solvents. *Langmuir* **2010**, *26*, 183-190.
- (24) Gao, S.; Moran, K.; Xu, Z.; Masliyah, J. Role of Naphthenic Acids in Stabilizing Water-in-Diluted Model Oil Emulsions. *J. Phys. Chem. B.* **2010**, *114*, 7710-7718.
- (25) Schramm, L. L.; Stasiuk, E. N.; Yarranton, H.; Maini, B. B.; Shelfantook, B. Temperature Effects from the Conditioning and Flotation of Bitumen from Oil Sands in Terms of Oil Recovery and Physical Properties. *J. Can. Pet. Technol.* **2003**, *42*, 55-61.
- (26) Gu, G.; Xu, Z.; Nandakumar, K.; Masliyah, J. Effects of Physical Environment on Induction Time of Air-bitumen Attachment. *Int. J. Miner. Process.* **2003**, *69*, 235-250.
- (27) Ren, S.; Trong, D. V.; Zhao, H.; Long, J.; Xu, Z.; Masliyah, J. Effect of Weathering on Surface Characteristics of Solids and Bitumen from Oil Sands. *Energy Fuels* **2009**, *23*, 334-341.
- (28) Feng, X.; Mussone, P.; Gao, S.; Wang, S.; Wu, S. Y.; Masliyah, J. H.; Xu, Z. Mechanistic Study on Demulsification of Water-in-Diluted Bitumen Emulsions by Ethylcellulose. *Langmuir* **2010**, *26*, 3050-3057.
- (29) Li, Q.; Jonas, U.; Zhao, X. S.; Kapp, M. The Forces at Work in Colloidal Self-Assembly: A Review on Fundamental Interactions between Colloidal Particles. *Asia-Pac. J. Chem. Eng.* **2008**, *3*, 255-268.
- (30) Butt, H.; Graf, K.; Kappl, M. In *Physics and Chemistry of Interfaces*; Wiley-VCH: Weinheim, **2003**.

- (31) Liu, J.; Xu, Z.; Masliyah, J. Interaction Forces in Bitumen Extraction from Oil Sands. *J. Coll. Inter. Sci.* **2005**, *287*, 507-520.
- (32) Liu, J.; Xu, Z.; Masliyah, J. Studies on Bitumen-Silica Interaction in Aqueous Solutions by Atomic Force Microscopy. *Langmuir* **2003**, *19*, 3911-3920.
- (33) Berg, J. C. In *An Introduction to Interfaces & Colloids: The Bridge to Nanoscience*; World Scientific: Singapore, Hackensack, NJ, **2010**.
- (34) Wang, Y.; Jia, W.; Ding, M.; Yang, H.; Hu, B.; Ren, S. Effect of Diluent Addition on Bitumen Liberation from a Glass Surface. *Energy Fuels* **2012**, *26*, 1019-1027.
- (35) He, L.; Lin, F.; Li, X.; Xu, Z. Enhancing Bitumen Liberation by Controlling the Interfacial Tension and Viscosity Ratio through Solvent Addition. *Energy Fuels* **2014**, *28*, 7403-7410.
- (36) Zhao, H.; Trong Dang-Vu; Long, J.; Xu, Z.; Masliyah, J. H. Role of Bicarbonate Ions in Oil Sands Extraction Systems with a Poor Processing Ore. *J. Dis. Sci. Tech.* **2009**, *30*, 809-822.
- (37) He, L.; Lin, F.; Li, X.; Xu, Z.; Sui, H. Effect of Solvent Addition on Bitumen–Air Bubble Attachment in Process Water. *Chem. Eng. Sci.* **2015**, *137*, 31-39.
- (38) He, L.; Lin, F.; Li, X.; Xu, Z.; Sui, H. Enhancing Heavy Oil Liberation from Solid Surfaces using Biodegradable Demulsifiers. *J. Environ. Chem. Eng.* **2016**, *4*, 1753-1758.
- (39) Stanislaus, A.; Marafi, A.; Rana, M. S. Recent Advances in the Science and Technology of Ultra Low Sulfur Diesel (ULSD) Production. *Catalysis Today* **2010**, *153*, 1-68.

- (40) Ivanova, L.; Koshelev, V.; Burov, E. Influence of the Hydrocarbon Composition of Diesel Fuels on their Performance Characteristics. *Pet. Chem.* **2014**, *54*, 466-472.
- (41) Brient, J. A.; Wessner, P. J.; Doyle, M. N. In *Naphthenic Acids*; Kirk-Othmer Encyclopedia of Chemical Technology; John Wiley & Sons, Inc. **2000**.
- (42) Hao, L.; Jiang, B.; Zhang, L.; Yang, H.; Sun, Y.; Wang, B.; Yang, N. Efficient Demulsification of Diesel-in-Water Emulsions by Different Structural Dendrimer-Based Demulsifiers. *Ind. Eng. Chem. Res.* **2016**, *55*, 1748-1759.
- (43) Arik, E.; Altan, H.; Esenturk, O. Dielectric Properties of Diesel and Gasoline by Terahertz Spectroscopy *J. Infrar. Milli. Terahz. Wav.* **2014**, *35*, 759-769.
- (44) Xu, J.; Zhang, H.; Zhang, J.; Yang, D.; Qian, J.; Liu, L.; Liu, L. The Determination of Diesel Density and Refractive Index by Near Infrared Spectroscopy. *Pet. Sci. Tech.* **2013**, *31*, 2489-2493.
- (45) He, L.; Zhang, Y.; Lin, F.; Xu, Z.; Li, X.; Sui, H. Image Analysis of Heavy Oil Liberation from Host Rocks/Sands. *Can. J. Chem. Eng.* **2015**, *93*, 1126-1137.
- (46) Chen, T.; Lin, F.; Primkulov, B.; He, L.; Xu, Z. Impact of Salinity on Warm Water-Based Mineable Oil Sands Processing. *Can. J. Chem. Eng.* **2017**, *95*, 281-289.
- (47) Lambert, J. B.; Shurvell, H. F.; Lightner, D.; Cooks, R. G. In *Introduction to Organic Spectroscopy*; Macmillan Publishing Company, Collier Macmillan Publishers: New York, London, **1987**, Vol. 1.



- (48) Liley, P. E. Thermophysical Properties of Ice/Water/Steam from -20°C to 50°C. *Int. J. Mech. Eng. Edu.* **2005**, *33*, 45-50.
- (49) Esteban, B.; Riba, J.; Baquero, G.; Puig, R.; Rius, A. Characterization of the Surface Tension of Vegetable Oils to be used as Fuel in Diesel Engines. *Fuel* **2012**, *102*, 231-238.
- (50) Brient, J. A.; Wessner, P. J.; Doyle, M. N. In *Naphthenic Acids*; Kirk-Othmer Encyclopedia of Chemical Technology; John Wiley & Sons, Inc. **2000**.
- (51) Liu, J.; Xu, Z.; Masliyah, J. Interaction between Bitumen and Fines in Oil Sands Extraction System: Implication to Bitumen Recovery. *Can. J. Chem. Eng.* **2004**, *82*, 655-666.
- (52) Wen, W. W.; Sun, S. C. An Electrokinetic Study on the Oil Flotation of Oxidized Coal. *Sep. Sci. Tech.* **1981**, *16*, 1491-1521.
- (53) Liu, J.; Zhou, Z.; Xu, Z.; Masliyah, J. Bitumen–Clay Interactions in Aqueous Media Studied by Zeta Potential Distribution Measurement. *J. Coll. Inter. Sci.* **2002**, *252*, 409-418.
- (54) Liu, J.; Zhou, Z.; Xu, Z. Electrokinetic Study of Hexane Droplets in Surfactant Solutions and Process Water of Bitumen Extraction Systems. *Ind. Eng. Chem. Research* **2002**, *41*, 52-57.
- (55) Ali, L. H. Surface-Active Agents in the Aqueous Phase of the Hot-Water Flotation Process for Oil Sands. *Fuel* **1978**, *57*, 357-360.

(56) Fauth, D. J.; Frommell, E. A.; Hoffman, J. S.; Reasbeck, R. P.; Pennline, H. W. Eutectic

Salt Promoted Lithium Zirconate: Novel High Temperature Sorbent for CO<sub>2</sub> Capture. *Fuel*

*Process Tech.* **2005**, *86*, 1503-1521.

(57) Friesen, W.; Michaelian, K. H.; Long, Y.; Dabros, T. Effect of Solvent-to-Bitumen Ratio on

the Pyrolysis Properties of Precipitated Athabasca Asphaltenes. *Energy Fuels* **2005**, *19*,

1109-1115.